1999 NSREC

SHORT COURSE

SECTION IV

PROTON EFFECTS AND TEST ISSUES FOR SATELLITE DESIGNERS

Paul W. Marshall
Consultant

Cheryl J. Marshall
NASA/Goddard Space Flight Center

IV. Proton Effects and Test Issues for Satellite Designers

General Introduction

This portion of the Short Course is divided into two segments to separately address the two major proton-related effects confronting satellite designers: ionization effects and displacement damage effects. While both of these topics are deeply rooted in "traditional" descriptions of space radiation effects, there are several factors at play to cause renewed concern for satellite systems being designed today. For example, emphasis on Commercial Off-The-Shelf (COTS) technologies in both commercial and government systems increases both Total Ionizing Dose (TID) and Single Event Effect (SEE) concerns. Scaling trends exacerbate the problems, especially with regard to SEEs where protons can dominate soft error rates and even cause destructive failure. In addition, proton-induced displacement damage at fluences encountered in natural space environments can cause degradation in modern bipolar circuitry as well as in many emerging electronic and opto-electronic technologies.

A crude, but nevertheless telling, indication of the level of concern for proton effects follows from surveying the themes treated in papers presented at this conference. The table lists themes found in the IEEE Transaction on Nuclear Science (TNS) December issue from the past year and compares them with the December issue's content a decade earlier. Ten years ago there were nine papers, or about 10% of the total, dealing with the four indicated topics. At that time, single event effects from protons were the primary concern, and these were thought to be possible only when a nuclear reaction initiated energetic recoil atoms. This is shown in the table as the 'traditional" SEE subject. A decade later, submissions addressing this topic had doubled, while papers devoted to displacement damage studies had increased from one to nine! More importantly, displacement damage effects in the natural space environments have become a concern for degradation in modern devices (other than solar cells), and this was not so ten years earlier.

Table: Growth of concern for proton effects over the past decade

Topic	IEEE TNS, Vol. 35, No. 6, 1988	IEEE TNS, Vol. 45, No. 6, 1998
Environments	1	5
Dosimetry	4	2
Displacement Damage	1	9
"Traditional" SEE	3	6
New Effects		4
Total	9 (~10% of total)	26 (~30% of total)

In the recent Transactions, four papers were devoted to effects that were either unknown or considered unimportant a decade earlier. These include soft errors from direct ionization by protons [Mars-98, Reed-98] and from nuclear elastic scattering events [Ingu-97, Savage-98, Johnston-98], along with hard failure SEE mechanisms such as latch-up [Norm-98] and dielectric breakdown in power MOS devices [Titu-98]. The aggregate level of

concern is obvious with a total of 26 papers, or about one third of the articles, in the 1998 December TNS dealing substantially with proton-related issues.

In this Short Course segment we will attempt to survey the important developments that have taken place in the past few years. The material we cover emphasizes the developments affecting design tradeoffs for current satellite systems with the recognition that any given component can potentially be used so long as the risks are identified adequately and mitigated appropriately. We approach this task by citing the studies that identify the various effects that protons can have, and then by indicating and demonstrating the tools available to radiation effects experts and knowledgeable designers to quantify the associated risks.

To place the material in the context of the needs of the satellite design engineer, we offer the following list of reasons that might motivate the need for proton testing of a given device or circuit.

Reasons to test with protons:

1. Expect proton SEEs and have no satisfactory means of predicting response without proton test data.
   - Have no SEE data on part type and need to characterize for a proton rich environment
   - Have heavy ion SEE data and correlation approaches indicate "marginal" performance
   - Need to gain general idea of heavy ion sensitivity and have package penetration test issues
   - Suspect a sensitivity to direct ionization induced SEEs from protons (e.g., optocouplers)
   - Need to assess sensitivity to destructive failure (e.g., latch-up) from protons

2. Expect proton displacement damage and have no satisfactory means of predicting response without test data.
   - Have no displacement damage data on part type and need to characterize for a proton rich environment
   - Need to verify response on flight-lot devices where lot-to-lot variations can be large (e.g., COTS)
   - Have neutron data and correlation approaches indicate "marginal" performance
   - Need to measure a "damage function" energy dependence to reduce uncertainty associated with predictive tools
   - Mixed damage and TID from protons in application indicates need for proton tests

3. Need to assess TID response to proton-induced dose with high precision (e.g., calibration of p-MOS dosimeters)

Following the major division indicated in the above list, the subject material for this section of the course is divided into two segments with Part A devoted to ionization effects and Part B to displacement damage effects. The section on ionization effects addresses the environment and satellite configuration considerations to identify scenarios where proton dose can play an important role in TID effects. Proton-induced single event effects occurring from

either direct ionization or generation of reaction recoils will be included in this section, but the emphasis will be on more recent studies describing new sensitivities to proton-induced ionization events. The reader will be referred to previous Short Course notes and related literature for discussions of mechanisms and rate calculations for "traditional" proton SEE and TID concerns, with the exception of two case studies. These two studies examine special concerns for modern communications satellite constellations that route high-speed signals.

The section on displacement damage considers the numerous device types exhibiting sensitivity to displacement effects. The primary tools, like the concept of Non-Ionizing Energy Loss (NIEL), now used to treat proton-induced displacement effects have been mostly developed within the past decade. This section addresses the justifications, methodology, and associated uncertainties in applying these tools to various classes of Si-based devices as well as emerging III-V technologies for electronic and opto-electronic applications. Emphasis will be given to satellite environments, including shielding efficacy and tradeoffs.

Our goal is to capture the current understanding of the many proton-related concerns important to the satellite subsystem engineer. At the beginning of the first section on ionizing effects, a top-level treatment of the environments internal to satellites will be provided, along with references to previous Short Course discussions for additional detail. The emphasis of the remaining material throughout both sections is on the effects, tools, and associated information to enable informed tradeoffs of design options.

Section IV. Proton Effects and Test Issues for Satellite Designers

Part A: Ionization Effects

Paul W. Marshall
7655 Hat Creek Road
Brookneal, VA 24528

Cheryl J. Marshall
NASA Goddard Space Flight Center
Code 562
Greenbelt, MD 20771

SECTION IVA: IONIZATION EFFECTS

Paul W. Marshall and Cheryl J. Marshall

1.0 INTRODUCTION

This first segment covers various ways in which proton-induced ionization can affect circuit operation. For our purpose, this includes TID effects as well as both direct and indirect single event phenomena. Before addressing the device and circuit effects, we offer a brief overview of the near-Earth proton environments and issues impacting the environment description internal to the satellite. This section also provides examples and discusses issues concerning the generation of design requirements based on the expected environment. Following the environment section, we offer a brief discussion of proton-specific concerns for TID effects. Next, the fourth section examines soft errors due to protons, again with emphasis on recent developments, and the fifth section looks at hard errors.

2.0 PROTON ENVIRONMENTS FOR SATELLITES

Protons occur in every imaginable orbit with variations in spectral energy composition, arrival rates, and sometimes arrival trajectories. The three sources are trapped protons in the inner Van Allen radiation belt, the proton component of solar particle events, and hydrogen nuclei from intergalactic cosmic rays. Careful discussions of the near-Earth, interplanetary, and other planet proton environment models are available in the Conference Short Course notes from 1997 [Bart-97]. The interested reader should refer to those notes and the cited literature to gain an understanding of the characteristics and shortcomings of the widely used NASA AP-8 [Sawy-76] model for trapped protons, the CREME-96 [Tylk-96] cosmic ray model, and various descriptions of solar proton probability models. These models should be viewed only as working approximations aimed at describing the major features of the external environment with the recognition that both the subtleties and major features of the environments are the concern for numerous space-borne experiments and ongoing modeling efforts.

2.1 Environment Description and Issues

With regard to the range of proton environments and the factors affecting them, the basic models cited above are the predictive tools of the environment specialists. The 1997 Short Course by Janet Barth [Bart-97] offers an excellent discussion of these and several other models, their applicability, issues affecting their accuracy, and the proton environments as they change with orbital position and solar cycle period. Detailed treatment is outside the scope of this material, but in addition to those notes, interested readers may wish to locate the 1988 review article "The Natural Radiation Environment Inside a Spacecraft," [Stass-88] or this conference's Short Course notes on "Radiation Environments in Space" [Stass-90]. For quick reference, the general character of the trapped proton belts external to the spacecraft is provided here as figure 1.

AP8MIN EQUATORIAL OMNIDIRECTIONAL RADIAL PROFILES

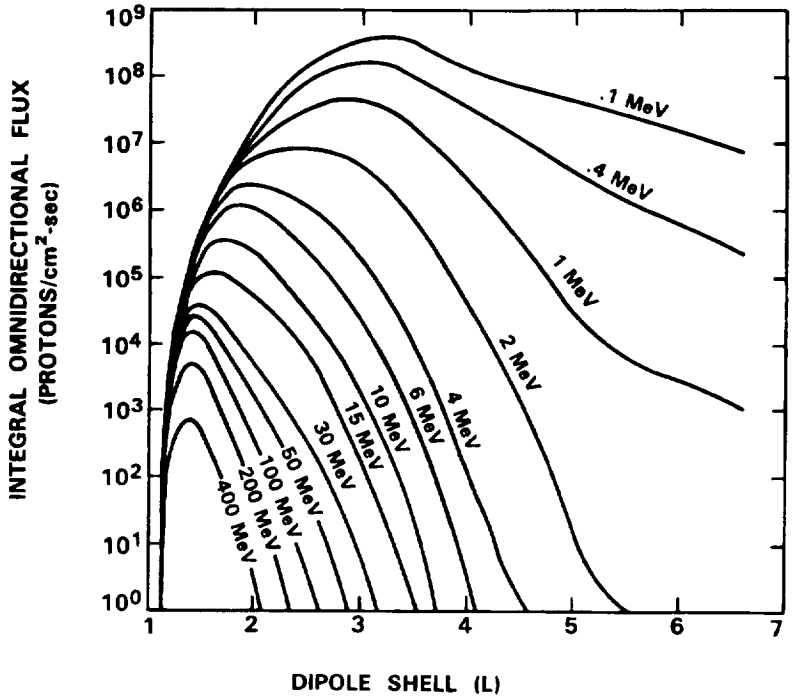

Figure 1. The AP-8 model for solar minimum conditions at 0 degrees inclination indicates the higher energy protons at lower altitudes [after Stass-88]. The orbit altitude in km is related to dipole shell as [(L x 6370 km)-6370 km] where 6370 km is the Earth's radius.

There is a document in development to supplement the various radiation models with practical considerations for satellite applications and make general trends more accessible to design engineers. The IEEE (Draft) Standard 1156.4 [IEEE-1156.4] document is aimed at establishing generic descriptions of four orbit categories: Low Earth Orbit (LEO) below about 10,000 km, Medium Earth Orbit (MEO) from 10,000 to 20,000 km, Geostationary Orbit (GEO) at 36,000 km, and transfer or Highly Elliptical Orbit (HEO). This document identifies example orbits in each of these categories and illustrates proton and other radiation characteristics of those orbits for the purpose of ionizing (but not displacement) effects in space-borne computers. Be warned though, that these are only examples and there is no justification to generalize from those orbits even to other orbits within the same category.

For the designer, detailed understandings of the environment models are fortunately not usually necessary. Instead, the proton and other radiation related requirements are either supplied by the procuring organization or generated "in house" by resident radiation environment experts. Several years ago, it was not uncommon to see radiation design specifications expressed in terms of total ionizing dose (or depth-dose curves) supplemented with either Linear Energy Transfer (LET) spectra or guidance with respect to LET threshold for single event induced hard errors and upset rates from cosmic rays. Proton contributions to

the depth-dose may have been identified, but often there was no breakout of the expected proton energy spectra and fluxes. In many cases, it was assumed that components that could be upset by protons would be screened out by the requirement for a high threshold LET for cosmic ray effects.

With today's emphasis on high performance systems and the component selections now available, all that has changed. Now a more reasonable assumption would be that proton effects are expected, and part of the designer's task is to manage the associated risk. Increasingly, it is the responsibility of the design team to assess radiation-related risk, and proton effects are often an important part of this equation. There is still quite a variation in the level of detail called out in the proton environment description provided to the design effort. It usually contains some, but rarely all, of the following elements:

1. trapped proton total ionizing dose contribution to a depth-dose relation
2. trapped proton energy spectra behind typical shield thickness
3. peak trapped proton flux with energy composition (in orbit "hot spot")
4. average daily trapped proton flux
5. mission fluence for protons > 25 MeV (or some other cutoff)
6. solar particle event (SPE) proton energy spectrum with fluence per mission
7. peak (worst case) proton flux from SPE with energy composition
8. assumed frequency of occurrence of design case SPE
9. cosmic ray LET spectrum including proton contributions
10. variations on each of the preceding to reflect solar cycle related changes
11. variations on each of the preceding to reflect uncertainties and design margins

There are no standardized formats for identifying either the proton environments or the radiation-related requirements for proton effects. The preceding list offers several environment descriptions that are commonly seen in various combinations. Often, the intention is to identify TID levels, a mission-duration proton spectrum for SEE and possibly displacement damage concerns, and a peak flux (or fluxes) for use in assessing peak SEE rates. Item ten in the list touches on the often seen practice of inflating the expected environment to add margin for various reasons, ranging from uncertainties in environment models to part-to-part response non-uniformity and response uncertainty. Margin will be discussed in a later section.

In practice, the environments identified in many requirements documents do not always adequately specify the details needed to properly assess proton-related effects. This situation follows, in some part, from a natural lag between the identification of a given important effect (e.g., displacement damage in optocouplers, or proton upset response best described by a two parameter Bendel formalism as discussed later) and the recognition of the need to include detailed proton spectral information rather than just proton-induced rad(Si) and > 25 MeV fluences. Also, the timeline associated with procuring flight hardware may result in periods of years between the definition of the orbit environment description to the detailed design, and new effects, which may emphasize previously unimportant aspects of the environment, are continually identified. From the radiation effects perspective, it's hard to overdo the level of detail in the environment description called out in a requirement.

2.2 Example Proton Environment Description

As an example of the proton environment description in a program currently under way, the interested reader may examine the document SSP 30512 Rev. C entitled "Space Station Ionizing Radiation Design Environment" [SSP-30512]. This document, released in June of 1994, describes the ionizing radiation environment as calculated for the International Space Station Alpha (ISSA) at an altitude of 500 kilometers and inclination of 51.6 degrees. Five years later, it remains the reference environment description for hardware currently being designed for ISSA, and it has general applicability to the multi-national and multi-agency effort. We include this example because this program is of general interest and also because the proton environment description is unusually thorough.

The descriptions of various proton environments for ISSA are contained in table 1. The first item accounts for most of the protons encountered in the low-Earth orbit. Though not indicated explicitly in any of the ten items, most of these protons will be encountered during passes through the South Atlantic Anomaly (SAA). The average daily proton flux predicted in this table is calculated by using the AP-8 model for solar maximum conditions and shown below in integral form as figure 2.

In table 1 the second and third listings address the depth-dose relation and are included here since protons account for a portion of the total ionizing dose. Figure 3 shows the relative annual dose contributions for electrons and protons at the center of a solid aluminum sphere. The chart indicates how protons dominate the TID for shield thicknesses greater than about 200 mils Al, and this result is typical of most orbits that encounter the trapped proton belts. Careful inspection of the proton curve illustrates how ineffective shielding is for stopping protons. Note the steep falloff in the electron dose with increasing depth and the relatively flat character of the proton curve. Increasing the shield thickness form 100 to 1000 mils only reduces the resulting dose by about 50%. For this reason, and others discussed later, shielding is often not the best technique for minimizing proton effects.

Table 1: List of tables describing proton-related environments for ISSA [SSP-30512]

Item	Table	Description
1	3.1.1-2	AP8MAX differential and integral flux energy spectra for trapped protons
2	3.1.2-1	One year dose at the center of a solid aluminum sphere (rads(Si))
3	3.1.2-2	One year dose in semi-infinite aluminum medium (rads(Si))
4	3.2.1.1-1	Daily average internal proton integral flux spectrum
5	3.2.1.1-2	Daily average internal proton differential flux spectrum
6	3.2.1.2-1	SAA pass internal peak proton integral flux spectrum
7	3.2.1.2-2	SAA pass internal peak proton differential flux spectrum
8	3.2.1.4-1	Combined integral flux LET spectra (WI[1]=4) no solar flare flux
9	3.2.2-1	Maximum solar flare peak proton integral flux spectrum
10	3.2.2-2	Maximum solar flare peak proton differential flux spectrum

[1] WI = weather index

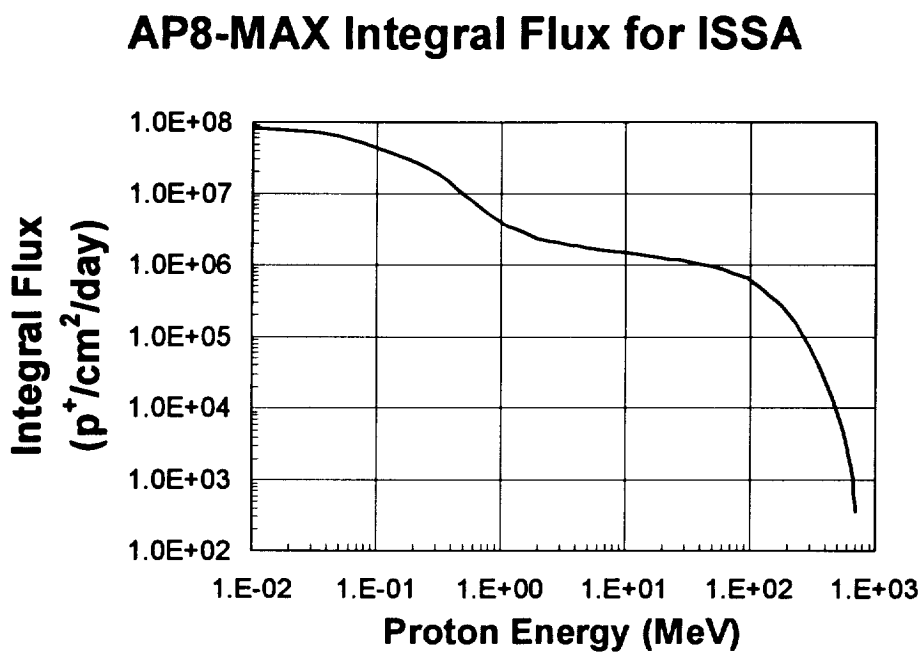

Figure 2. Integral daily proton flux for the example International Space Station Alpha orbit of 500 km x 51.6 degrees shows the large numbers of low energy protons that are easily shielded. Fluxes in the tens to hundreds of MeV can penetrate to sensitive components resulting in single event effects and both ionizing dose and non-ionizing dose.

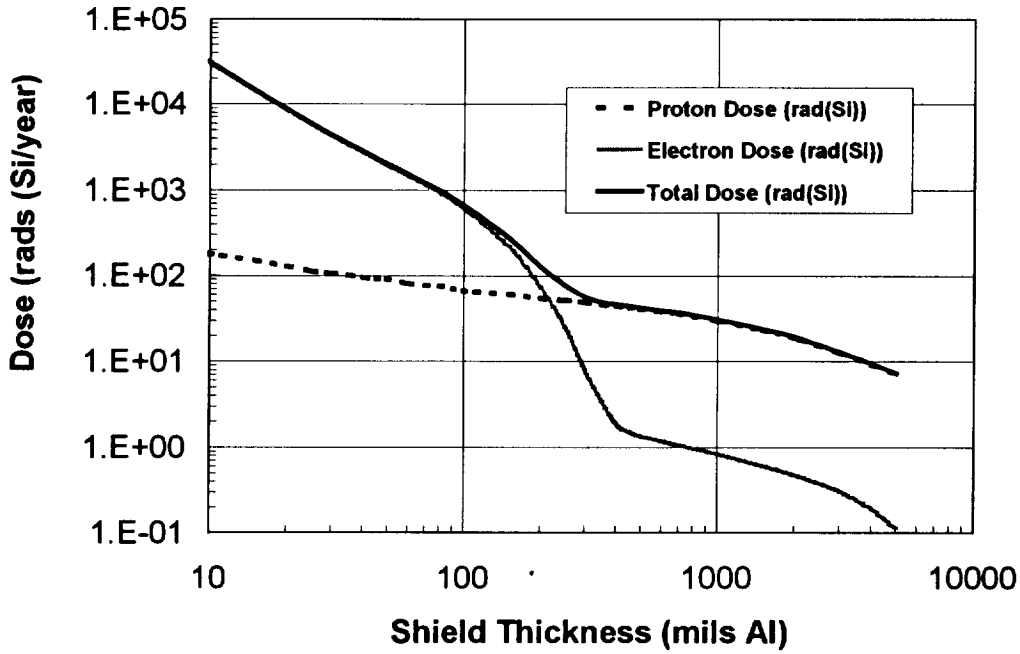

Figure 3. For the 500 km x 51.6 degree orbit for ISSA, the dose from trapped protons dominates for Al shield thicknesses above 200 mils. With increasing shield thickness, the average proton energy increases.

The fourth and fifth items in table 1 provide detailed information on spectral energy composition for aluminum shield thicknesses of 0, 50, 500, 1000, 2000, 4000, and 7000 mils. The inclusion of predictions for very thick shielding is appropriate for the manned bays in ISSA, but is atypical for unmanned vehicles. Items six and seven in table 1 address the peak proton flux expected from trapped protons during passages through the South Atlantic Anomaly. Note that the peak flux occurring due to trapped protons is almost always lower than the peak flux due to solar particle events, with the exception being low inclination LEO orbits. However the SAA is encountered on about 50% of ISSA orbits (several times a day) as opposed to the relatively rare solar events. In this case, the peak from SAA trapped protons, integrated over energies > 10 MeV, is 2.04×10^3 p/cm^2/s, which is 54 times the orbit-averaged rate. Table 1, items nine and ten describe the modeled peak rates corresponding to solar particle events, including effects of the Earth's geomagnetic shielding. Data listed in these tables indicate an expected peak (for design purposes) of 3.36×10^5 p/cm^2/s. This is 165 times the peak rate during SAA passages. This event would be expected, as described in [SSP-30512], once per 11 year solar cycle, or approximately once per mission for ISSA.

Peak proton arrival rates for a given mission cannot be predicted in a deterministic manner. The use of the October 1989 flare as a design environment, shown in figure 4, for ISSA is a somewhat arbitrary choice. Other options exist, including other peak solar particle models incorporated in CREME-96 [Tylk-96, Tylk-96a]. More recently, a probabilistic model for predicting peak flux based on solar cycles 20, 21, and 22 has been proposed [Xaps-98], and this allows a more quantitative approach to assessing the risk of exceeding a given proton flux. Please see the discussion of peak SPE proton rates in the 1997 Short Course notes [Bart-97] for more information and discussion on this topic.

The eighth table entry (combined integral flux LET spectra (weather index=4) no solar flare flux) describes the cosmic ray design environment for ISSA in terms of the LET spectrum from heavy ions. We acknowledge that for orbits encountering the trapped proton belts there are relatively few cosmic ray protons. However, for devices (e.g., detectors) sensitive to single events from proton ionization, cosmic ray protons may be a concern. Hydrogen ions (protons) are after all the most abundant constituent of the composite cosmic ray spectrum, and they account for 83% of all cosmic rays outside the effects of the Earth's magnetic field. Figure 5 indicates the composite LET spectrum with two shield thicknesses for ISSA. In terms of LET, protons account for only about 1 in 10^5 incident particles at the lowest LET value shown in the figure (0.1 MeVcm^2/mg). Though not shown, at LET values of 0.01 MeVcm2/mg and 0.001 MeVcm^2/mg proton contributions increase to 0.5% and 88% respectively. If lower LET values are important, then the proton component of cosmic rays may dominate. Most cosmic ray protons are very energetic and shielding has little effect.

For the ISSA environment definitions, proton spectra are provided with various shield thicknesses. Not all design efforts provide this level of detail, and it is often necessary to modify the provided spectra to evaluate the detailed effects of additional shielding. Several transport code based routines are available to provide spectra and sometimes dose behind additional shielding. The capability and complexity of these tools cover a broad range from transport through relatively simple spherical or slab single thickness to full-up ray tracing and

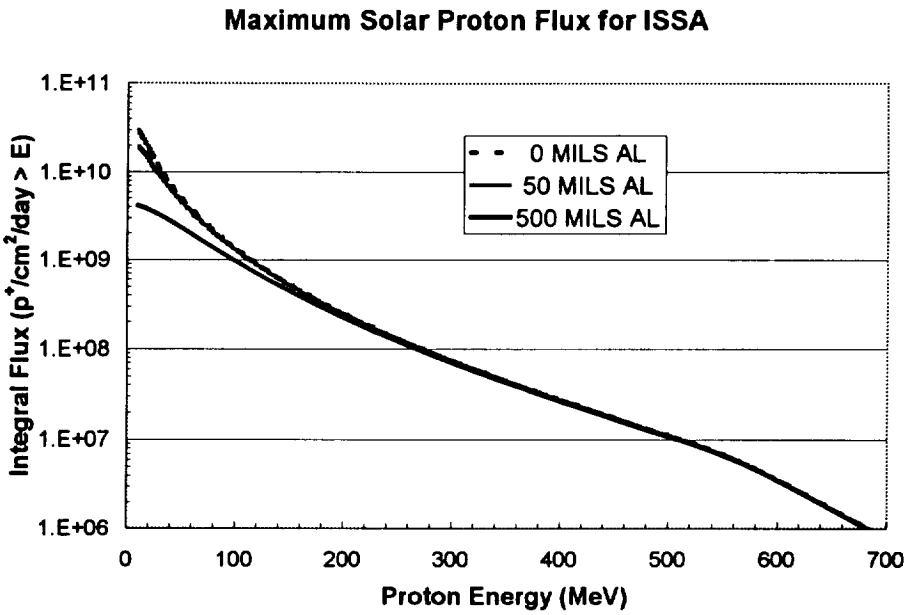

Figure 4. Peak solar proton flux from the October 1989 event, as propagated into the 500 km x 51.6 degree Space Station orbit, shows that less than a third of the protons reaching that orbit are stopped by 50 mils Al shielding. Also note that some protons above 400 MeV are present, in contrast to the trapped belt models.

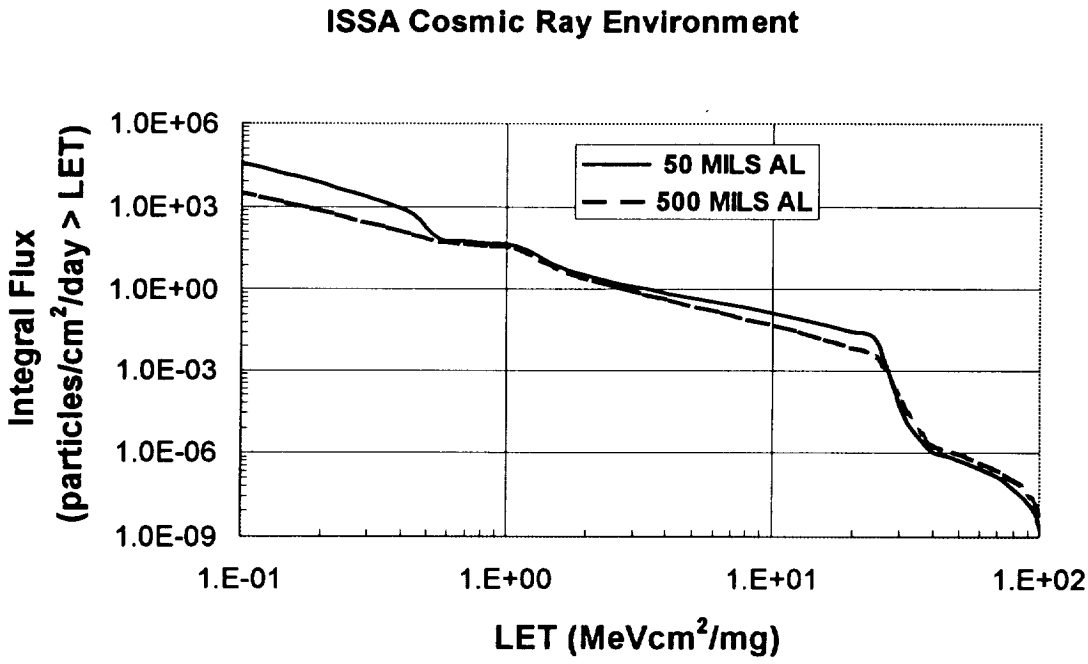

Figure 5. Proton contributions to the cosmic ray environment at 500 km and 51.6 degrees are included in the heavy ion LET spectrum. They account for 87% of all particles at an LET of 0.001 MeVcm^2/mg, but only .002% at the lowest LET shown in the chart.

high-density sector calculations. Additional discussion and a list of references are provided in the 1998 Short Course notes from this conference in section V part 3.1 [Kinn-98]. These tools play an important role in determining the dose or associated proton spectra at the box and component level. Usually, after surrounding boxes and satellite structural elements are considered, the resulting exposure at the subsystem and device level is less than that for a 100 mil Al spherical shield. However, the protection offered by structural shielding is of much less benefit than in the case of electron exposure because of the penetrating nature of protons.

2.3 Requirements: Proton Specific Issues

Expressions of requirements vary greatly from program to program. Top level requirements usually address performance of a system in a specified environment in terms of system lifetime, availability to perform mission objectives, and accuracy in meeting those objectives. At this level proton effects, along with other radiation effects, are only part of the reliability picture. From this level, system engineers usually arrive at a set of derived requirements that are applied to individual subsystems. These will likely address destructive failures, TID failure levels, and possibly soft error rates. Most often proton effects are lumped together with associated effects from other radiation sources. More recently, with the increasingly important role of displacement effects, proton levels may be specified explicitly for component types known to be susceptible to proton-specific effects, such as optocouplers, Charge Coupled Devices (CCDs), and others.

2.3.1 Total Ionizing Dose: TID requirements for a given mission are usually based on the composite electron-proton dose based on the depth-dose relation for the given mission. TID evaluations are customarily made using Co-60 test facilities with the assumption that there is a linear superposition of dose from protons and electrons (this assumption will be examined in a section IVA.3).

2.3.2 Destructive SEE: Similarly, for the case of single events effects resulting in hard failure, requirements for proton-related failure modes are rarely specified separately from heavy ion induced failure, though they sometimes should be. In practice however, extreme measures are usually taken to avoid hard failure, including the requirement that hard failures (e.g., latch-up) may not occur below the iron cutoff (or some higher LET value) of the heavy ion LET spectrum. If such measures are taken, then proton-induced hard failure will also be avoided, since proton sensitivity to SEEs is not expected where such high LET threshold values apply. Unless such assurances are in place, we suggest that requirements should be written to address the possibility of hard failures due to protons. In LEO applications of commercial power MOSFETs, for example, flight data has demonstrated that burnout is much more probable from protons than from heavy ions, even though the orbit inclination is 70^0 [Bart-98]. Expression of a requirement in terms of only LET would therefore be inadequate. Associated issues will be addressed in section 4.3.2 on Single Event Burnout (SEB).

2.3.3 Nondestructive SEE: It is more common for requirements to address proton-induced soft errors, at least indirectly, through the expression of requirements for average and peak error rates. Historically, this issue arose due to soft errors in memories, but in recent years the

literature (and unpublished flight data) provides many cases of microprocessors, ASICs, linear circuits, ADCs, detectors, and other components which exhibit sensitivity to soft errors from protons. Typically, requirement documents call for a level of performance, and it is the job of the box manufacturer to allocate error rates due to various expected sources. For orbits encountering the inner belts, protons often dominate average soft error rates in technologies sensitive to their effects. Where error rates are required to stay below some allowed maximum, the peak trapped proton flux and peak solar particle event fluxes represent the greatest challenges. For orbits outside of the proton belts, such as geostationary at 36,000 km, average proton arrival rates may be extremely low, but proton upset sensitivity can be a design driver with the infrequent solar particle event in mind.

2.3.4 Margin: Design margins arise from a variety of concerns and are expressed in a variety of ways, with some of these concerns specific to protons. Where large uncertainties exist either in the ability to predict the environment with high confidence or in the ability to predict circuit response, margin is applied to mitigate risk. In fact, the degree of margin is often scaled according to the criticality of the function being performed with the idea that survival is most important and some mission objectives are more important than others [e.g., Gate-96].

One of the sources of uncertainty is in the environment models. As an example, for trapped protons, the 23 year old AP-8 model has served to establish average and peak proton fluxes as well as proton dose for the radiation belts. The uncertainty associated with that model is stated to be a factor of two for long term orbit averages and higher for short duration periods (e.g., less than 1 year) [Sawy-76]. Therefore, it is appropriate to either double the predicted trapped particle environment or impose margin on the ability of the system to perform in the predicted environment. System designers frequently employ either approach. New information impacting the uncertainty of the AP-8 model is discussed in section 2.4.

Uncertain device response and the inability of imperfect predictive models to accurately describe performance also call for radiation design margin. These factors can be quite large, especially where the key variables governing device response are not well understood. In the portion of this Short Course segment concerning displacement damage we will illustrate this point for the cases of CCD damage and optocoupler degradation. Design margins of over two are warranted in each of these situations.

After factoring in more customary arguments for margin (e.g., part-to-part and lot-to-lot differences in response) the suggestion of additional factors of two or greater for each of these other proton specific sources usually comes as quite a shock to the design engineer. Resolution of these issues varies from program to program, usually with some element of compromise and the hope that either the components easily meet the requirements with margin or the design can be modified to accommodate the anticipated degradation. It is important that both the radiation effects specialist and the design engineer realize the needs for margin and not fall into the trap of assuming that the factor of 2 applied for environment uncertainty also accommodates uncertainties from other sources such as the response model.

2.3.5 Nonstandard Parts and Waivers: Every flight project design effort tracks parts that do not meet requirements with margin or that require "special" considerations. Often,

additional testing is required and special considerations are needed to evaluate risk. Nowadays, with the emergence of displacement damage concerns in Light Emitting Diodes (LEDs), optocouplers, and CCDs, many proton radiation effects are dealt with in this forum.

As specifications of proton environments and requirements improve, along with predictive models for the environments and device responses, these issues will likely be dealt with on a more routine basis and factors indicating needs for large design margins can be minimized. However, for now, many proton effects are only beginning to work their way into the concerns of the typical design effort. Proton testing is still viewed as an expensive alternative to be used sparingly. In many cases the details of defining proton test approaches and deciding on acceptable margins falls within the scope of "nonstandard parts evaluation" efforts. Resolution of these issues can present a significant set of interesting challenges.

2.4 Recent Updates to the Proton Environment Models

The preceding discussions have identified many of the proton environment models now being used, and indicated references for additional information. There are however a few key points to make regarding the dynamic status of the environment models. Janet Barth, in the 1997 Short Course notes [Bart-97], includes a section entitled "Problems with the AP-8 and AE-8 Models," and she follows this with a section entitled "Dynamic Models, A Beginning." These notes are well worth reading to see the path toward revisions to the existing NASA models.

Last year, at this conference, Houston and Pfitzer presented a paper entitled "A New Model for the Low Altitude Trapped Proton Environment," [Hous-98]. This "new model" is based on data acquired by instruments on the TIROS/NOAA spacecraft from 1978 through 1995. The key finding, from the satellite designer's perspective, is that the predicted fluxes are about twice as high as those from the AP-8 model, as indicated in figure 6. This finding seems to hold for proton energies of interest to satellite designers (> 16 MeV). The data cover the altitude range from 250-850 km. In conjunction with the CRESSPRO model [Meff-94], this significantly improves the empirical basis for major revision to the AP-8 model.

The probabilistic model for SPE peak *fluxes* presented at the 1998 NSREC has already been mentioned [Xaps-98]. Environment specialists also rely on a probabilistic modeling tool for predicting solar proton *fluences* during a mission [Feyn-96]. J. Feynman and co-workers at JPL have performed a statistical analysis including data on solar particle event proton fluences from the past three solar cycles. Their findings show that the largest events, such as the August-72 and October-89 events, belong in the same statistical distribution as other events. They provide a Monte Carlo based tool for assessing probability of exceeding a given fluence level during a specified mission duration. This model is especially important for geostationary and interplanetary missions, and it has rapidly gained acceptance.

The key point is that our understanding of even the gross features of the space radiation environment is not precise. Revisions and enhancements to the existing models are ongoing.

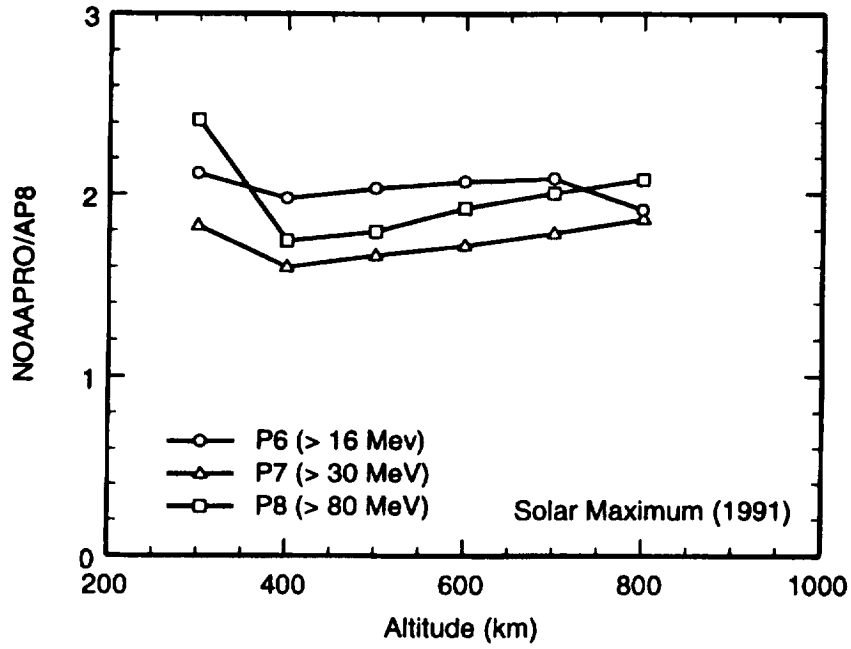

Figure 6. Recent dosimetry data from TIROS/NOAA satellites provide the basis for a revised model for trapped protons. The above figure and discussion in [Hous-98], by S.L. Houston and K.A. Pfitzer, indicate about twice the flux predicted by AP-8 for the three energy bins listed in the legend.

3.0 TOTAL IONIZING DOSE AND PROTONS

In this section we discuss several issues specific to total ionizing dose deposited by protons. Topics will include typical situations where proton-induced TID may be important to satellite systems, a discussion of the equivalence between proton dose and ionizing dose from other sources in the natural space environment, and finally a discussion of microdosimetry issues specific to protons. The emphasis will be on ionizing dose with the recognition that protons also deposit non-ionizing dose, which causes displacement damage. That is treated in the segment IVB of these notes.

3.1 Proton-Induced Total Ionizing Dose: Mechanisms and Issues

As protons traverse a solid, their positive charge presents an electrostatic force to the orbital electrons of the surrounding material. Excited electrons are freed from their bound state thereby creating electron-hole pairs. Some of these electrons (called delta rays) are liberated with sufficient energy to interact with other electrons at some distance from the incident proton's trajectory, thereby leading to an ionization track with some structure. This coulombic scattering process liberates electron-hole pairs at a rate that depends on the proton energy and also on the material it traverses. In Si, for example, the electron-hole pair creation requires (on average) 3.6 eV in energy from the incident proton. This empirically determined value is referred to as the ionization potential, and it depends on a number of factors including the material band-gap for the case of semiconductors. In insulators, ionization potentials are significantly larger, e.g., ~ 17 eV in SiO_2.

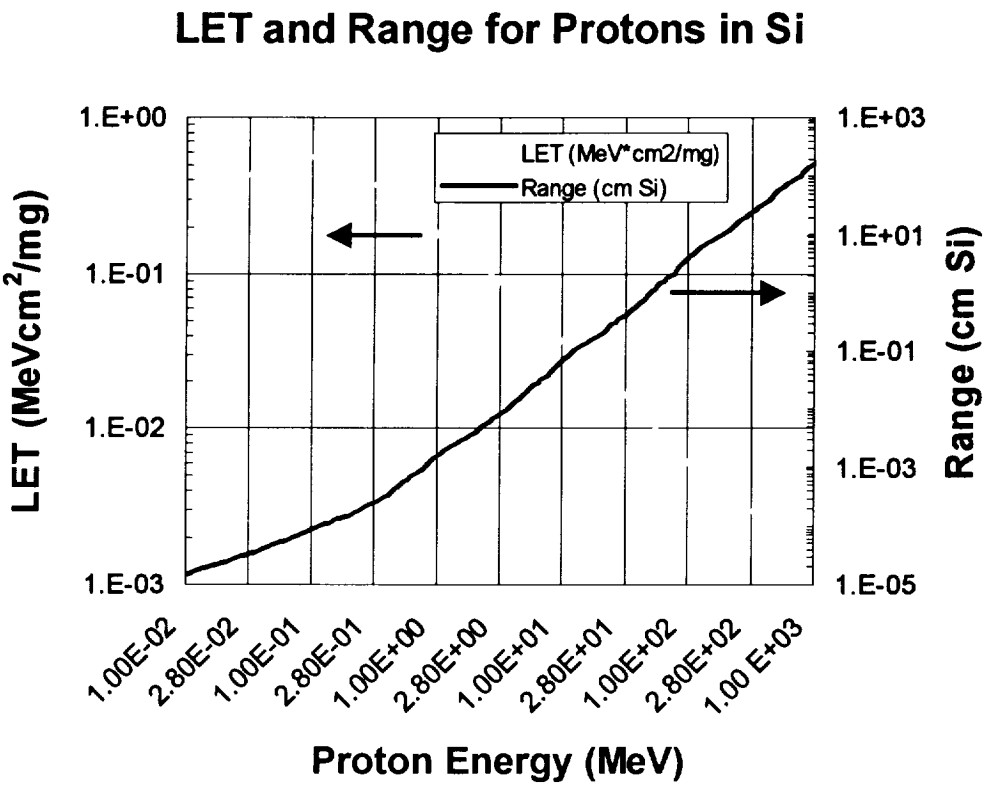

Figure 7. Lower energy protons with higher LETs are effectively stopped in satellite structural materials due to their short ranges. Higher energy protons are very penetrating, but fortunately transfer their energy at a lower rate. These relations do not address nuclear reactions occur for higher energy protons (>10 MeV) with a probability of about 10^{-5} for a pathlength of a few microns in Si.

The rate of energy loss for a proton (or any heavy ion) is termed the Linear Energy Transfer (LET) or stopping power, and the usual units are $MeVcm^2/mg$ though it can be converted to energy per unit pathlength by multiplying by the target material density. Again, this is an empirically determined relation, and its dependence on proton energy, known as the specific ionization curve, is shown in figure 7 along with the relation between proton range and energy. Note that the LET tends to decrease with increasing energy in the MeV regime encountered within satellites. Also, as the proton loses energy, the decrease in range is highly nonlinear. These energy loss kinematics are the basis for the situation in which the low energy protons are preferentially stopped by spacecraft materials. When the naturally occurring spectrum encounters satellite materials, protons at all energies lose energy, but the mean proton energy reaching the payload electronics actually increases with increasing shield thickness.

Along the trajectory of an individual proton, the path of ionization produces more and more electron-hole pairs per unit length until the proton approaches the end of its range. The LET actually peaks at an energy of about 80 keV in Si. This maximum in energy loss is often (inappropriately) referred to as the Bragg peak.

The precise details of energy loss are beyond the scope of this discussion, but it should be noted that proton dose is deposited along ionization tracks. On a micro-dosimetry scale the presence of these tracks leads to dose deposition that is therefore highly nonuniform in nature. In the following sections, ionization effects to electronic materials will be discussed and the inherent non-uniformity of proton dose on the microdosimetric scale will be placed into perspective by making comparisons to electron (or Co-60) dose deposition, which is much more uniform in nature.

Finally, it should be noted that the coulombic electronic scattering mechanism is by far the dominant mechanism for ionization purposes and for affecting proton energy loss, but other processes do occur. Nuclear elastic and inelastic processes lead to some ionizing dose deposition, but these are orders of magnitude down from electronic scattering. By far their most important role in electronic materials is in imparting non-ionizing energy leading to atomic displacements. These processes are discussed in detail in *Part B* of this Short Course section.

In the previous section on environments, it was noted that protons are encountered in all orbits. However, protons are significant contributors of TID only in certain cases. As indicated in figure 3, from the ISSA example in low-Earth orbit, the relative contribution of proton to electron dose increases with increasing shielding. The exact thickness at which proton dose becomes important varies with orbit. Proton dose may be a concern for low-Earth orbits or highly elliptical orbits that encounter the inner Van Allen belts, for orbits encountering high fluences from Solar Energetic Particle (SEP) events, or for missions reaching proton belts surrounding other planets. For circular orbits between about 1,500 and 5,000 km (the heart of the belts) the multi-year mission doses from protons can easily exceed 100 krad(Si). Whether in an orbit dominated by protons or one with mixed electron/proton exposures, the components most sensitive to TID effects are often buried deep in the spacecraft or protected with spot shielding. Consequently they may receive a substantial fraction of their dose from protons.

3.2 Is a rad always a rad?

The widely accepted unit for total ionizing dose from ionizing radiation is the rad (from Radiation Absorbed Dose). The rad is defined as 100 ergs per gram of energy absorbed in the exposed material, and 100 rads is equal to 1 Grey (Gy). For the case of heavy ions (including protons), the exposure in rads is determined from the ion LET and the particle fluence according to equation 1. Note that the LET and corresponding dose for a given particle fluence are material dependent quantities. As an example, a 100 MeV proton has an LET in silicon of 5.93 x 10^{-3} MeVcm^2/mg. For a fluence of 1 proton per square centimeter, the corresponding dose would be 9.5 x 10^{-8} rad(Si). This relation is depicted versus proton energy as figure 8.

$$\left(LET(matl.)\frac{MeV\cdot cm^2}{mg}\right)\cdot\left(fluence\cdot\frac{1}{cm^2}\right)\cdot\left(1.60\cdot10^{-5}\cdot\frac{mg\cdot rad}{MeV}\right)=X\cdot rad(matl.) \qquad [1]$$

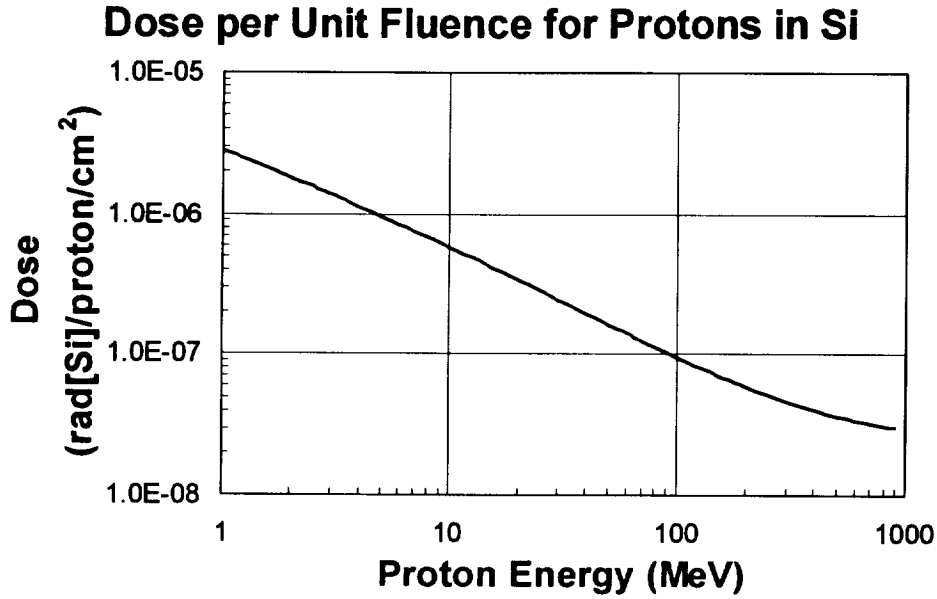

Figure 8. On average, each proton deposits dose according to its LET and the relation expressed in equation 1. The dependence in the above figure describes dose deposition from protons in silicon.

The basis for the use, or even the existence, of the rad is that the effects of the ionizing radiation in question, whether it be electrons, photons, protons, or other ions, will be equivalent for a given amount of adsorbed dose, irrespective of the radiation source. The radiation effects community has examined this assumption for several important cases, for example, the equivalence of 10 keV x-rays and Co-60 dose and the role of secondary electronic equilibrium at material interfaces. In the following paragraphs, we consider two microdosimetry issues that are specific to proton dose.

3.2.1 Lateral nonuniformities (LNUs): The term LNU in the context of radiation damage in MOS transistors describes the nonuniform distribution of holes in gate oxides. The initial papers addressing the phenomenon are cited in [Frie-88]. This paper describes a detailed investigation of the causes and effects; especially the false indication of interface state production using the subthreshold method when applied under cryogenic conditions. All of the initial work assessed the role of LNUs in gate oxides that were exposed to either Co-60 gamma rays or 10 keV x-rays. In the paper by Frietag, et al., a statistical formalism for the analysis of microscopic fluctuations in dose was introduced and applied to describe the behavior of the subthreshold current.

The following year the microdosimetry formalism from [Frie-88] was invoked and modified to treat the problem of LNUs arising from proton damage using a two component model [Xaps-89]. Conceptually, the problem of nonuniform dose deposition from protons might be suspected to cause significant effects when small geometries are considered such as in thin gate oxides. After all, there is a track structure, at least in the initial dose deposition. While the data and analyses presented in [Xaps-89] do demonstrate measurable effects in sub-threshold leakage current stretch-out at 77° K, perhaps the most remarkable result of this body

of work lies in the fact that, at least to first order, the microdosimetric fluctuations in ionizing dose deposition from protons are unimportant to satellite electronics.

3.2.2 Electron-Hole Recombination: This issue concerns the fate of the electron-hole pairs produced as the proton loses energy in a material. For traditional TID effects, holes are the more important since either trapped oxide charge or interface state formation lead to parameter shifts in transistor performance. The unique characteristic of electron-hole production along ion tracks is that electron-hole pairs along ion tracks are in relatively close proximity to neighboring charge pairs as compared to those generated by photon or electron radiation sources.

This close proximity can affect the charge yield for a given dose deposition through two mechanisms: geminate recombination and columnar recombination. Both recombination processes are well documented in literature extending back to the early 1900's. For the case of protons incident on Si, [Oldh-84] established what is today recognized as the definitive study on these effects. This reference provides vectors to the relevant literature, including the model developed to assess these effects for ions simulating cosmic ray effects [Oldh-83].

The geminate recombination model applies to the situation in which electron-hole pairs are widely separated from other charge pairs and therefore more likely to interact and possibly recombine with each other. Columnar recombination applies to densely ionized tracks along which charge pairs are so dense, and recombination is as likely to occur with pairs initiated in separate events. Figure 9, reproduced from [Oldh-84], indicates the energy dependence of the two recombination models and shows comparisons with published data acquired on n-type silicon. The yield in figure 9 is fractional, and at high proton energies where the geminate model applies the yield is expected to be the same as with Co-60. Note that even at high proton energies the relative yield does not approach unity. Furthermore, at lower proton energies important to both space environments and to test facilities, the yield decreases dramatically with decreasing proton energy. Recall from figure 7 that the lower energies correspond to increased LET and therefore more densely ionizing track structure.

The importance of proton dose in LEO missions notwithstanding, there have been few carefully controlled comparisons of Co-60 versus proton-induced TID response. A discussion of much of the relevant data is found in [Ma-89]. Investigation into p-MOSFET dosimeter response to proton dose has indicated similar behavior to that reported in [Oldh-84], but with indications of correlation between charge yield and electric field strength [Augu-82]. Figure 10, which is reproduced from the later work, indicates the relation between threshold voltage shift and gate bias on 1100 angstrom thick oxides for several different radiations, including 37 MeV protons. In [Stap-85], a clear trend was noted in the threshold voltage shifts of p-MOS transistors for the case of heavy ions versus literature data on Co-60. However, the comparison between Co-60 and 62 MeV protons showed no significant difference at a dose of 10 krad(Si). Recent comparisons of modern p-MOS dosimeters indicate similar behavior with a possible slight reduction is high energy proton response versus that from Co-60 [Peas-99].

Three papers have reported comparisons of photon versus proton-induced dose in devices other than p-MOS dosimeters. A careful experimental and modeling effort into the

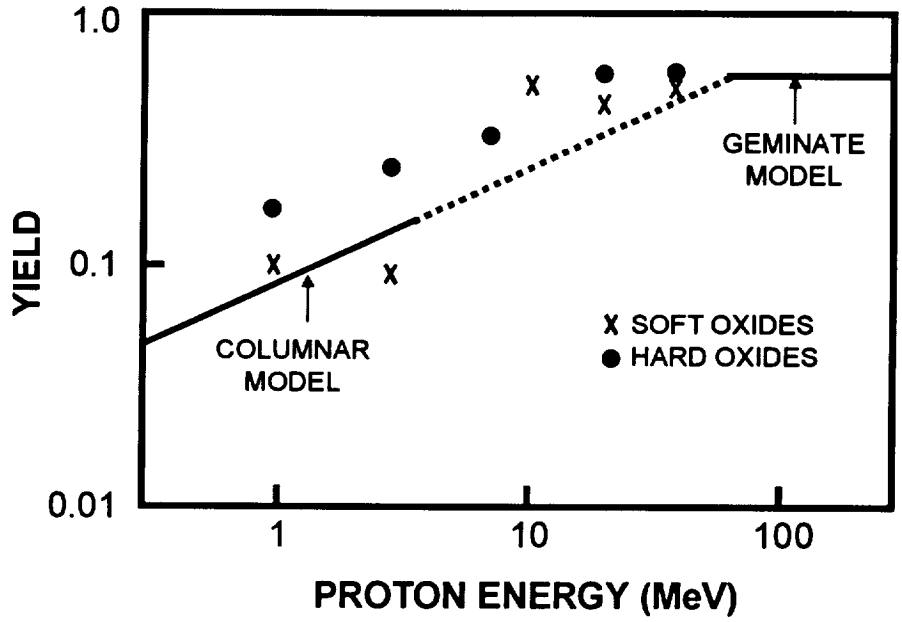

Figure 9. This figure is reproduced from [Oldh-84], and it indicates the energy dependence of the two recombination models. The yield is fractional, and at high proton energies where the geminate model applies the yield is expected to be the same as with Co-60

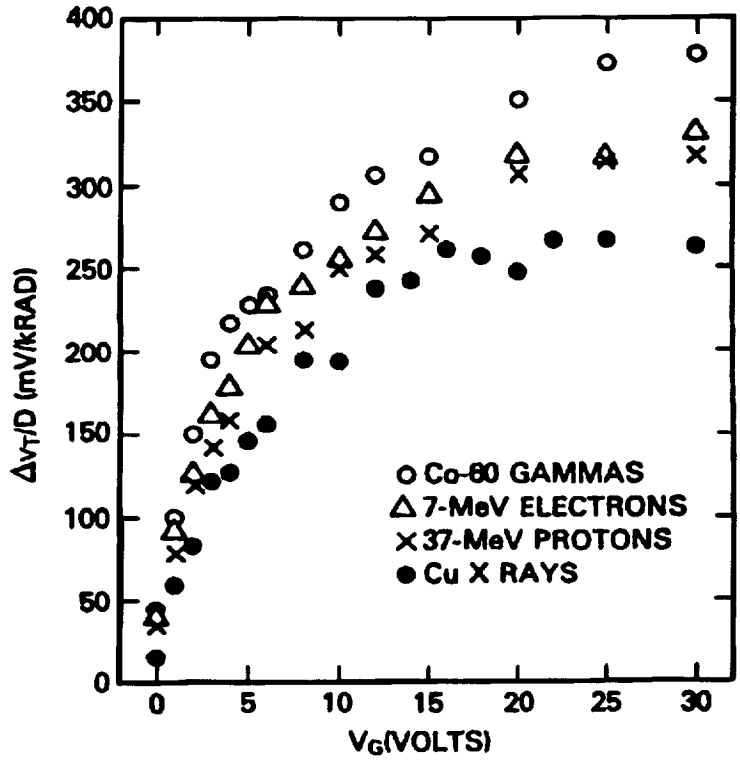

Figure 10. p-MOSFET dosimeter response to dose from proton and other sources indicates a correlation between charge yield and gate bias which affects electric field strength. The oxide thickness is 1100 angstroms.

response of radiochromic dye film dosimeters indicated the importance of the columnar recombination mechanism for protons [Hans-84]. This work also investigated track structure effects on charge yield and modeled these effects for protons from 3 to 16 MeV. [Xaps-90] reported a comparison of proton to Co-60 dose response of hardened gate oxides in terms of interface state buildup as measured by the sub-threshold technique. The data did not show a significant difference in response, and their work noted the high value of electric field as being a possible explanation for apparent dose equivalence.

There are three implications for the effects of recombination on the charge yield from proton exposures. First, the reduced effect per unit dose suggests that proton studies to assess TID effects should be approached very cautiously, especially if the intended application is in a mixed proton-electron environment, or worse, an environment dominated by electrons. The proton results could lead to slight underestimation of the environment effects. Secondly, if proton dose dominates in the application and the dose response is based on Co-60 studies, they may be slightly conservative. In the absence of detailed proton and Co-60 response comparisons on the parts being considered for flight, good engineering practice argues against factoring the reduced response to protons into the expected part lifetime. Finally, p-MOS dosimeters flown on board satellites may exhibit a reduced response to protons and therefore slightly underestimate the environment, unless the calibration is performed with consideration of the anticipated environment and the energy (and possibly field) dependence of the device response.

In summary, to first order, the concept of dose works well for assessing combined effects of various space radiation sources, including protons. In other words, 100 ergs per gram (1 rad) of energy deposition from one radiation source results in approximately the same device response as the same amount of energy deposited from another source. For TID purposes, LNUs from proton exposure do not appear to be an important effect. Geminate and columnar recombination lead to reduced charge yield, per unit rad, in proton environments. Even so, the assumption of a linear superposition of electron and proton dose, combined with Co-60 or 10 keV x-ray testing for component evaluations leads to reasonable estimates which may be slightly conservative in proton dominated dose environments. In closing, we would like to remind the reader that these comments address the fidelity of response estimated for proton-induced total ionizing dose only. If displacement effects are important, then there is no substitute for carefully planned tests, and x-ray or gamma ray testing is probably not appropriate. More will be made of this point in the section IVB on displacement effects.

4.0 PROTON-INDUCED SINGLE EVENT EFFECTS

The basis for the classic approach to single event effects from protons first appeared in [Guen-79]. Here, the upset mechanism description involved the proton (or neutron) initiating an inelastic nuclear reaction leading to high energy recoil atoms and subsequent localized ionization sufficient to cause upset. Proton upset in satellite microelectronics was not a major concern at first because of the larger feature sizes and correspondingly high critical charge required for upset. In time this would change, and within a few years, missions routinely saw upset rate increases corresponding to high proton fluxes. In the 1995 NSREC Short Course

segment on "Single Event Effects Qualification," Bill Stapor includes a list of 30 missions with confirmed proton-induced SEE experiences. Today, that list would be much longer.

In 1984 the key paper appeared, "Predicting Single Event Upsets in the Earth's Proton Belts" [Bend-84]. This semi-empirical model assumes the proton reaction based mechanism and allows the use of SEE test data at a single proton energy or multiple energies for the prediction of upset rates in the proton belts. In the single parameter model, the parameter relates the proton upset sensitivity to the proton energy threshold for upset production.

The basic formalism for proton-induced SEEs from nuclear reaction recoil products has not changed appreciably since its introduction in the mid-1980s. In 1989, a paper emphasizing application of the 2-parameter Bendel approach showed improved agreement with test data for modern devices with small feature size [Shim-89]. This was followed the next year by another paper advocating the 2-parameter approach and pointing out the importance of proton testing at higher energies to increase rate prediction accuracy [Stap-90]. In addition to the 1995 Short Course notes, the interested reader should refer to the 1997 NSREC Short Course segment on "Single Event Analysis and Prediction" by Ed Petersen [Pete-97]. This course offers an excellent discussion of proton upset mechanisms, models, and rate prediction tools, as well as practical consideration for proton upset cross section measurement. These course notes also provide detailed descriptions of the expanded range of component types for which proton SEEs are important. This includes not only memories, but also processors, ASICs, linears, and most modern circuit families. Additional related materials are found in Ed Petersen's review article on, "Approaches to Proton Single Event Rate Calculations," [Pete-96].

Given the level of discussion on the general topics of proton upset measurement and rate predictions in these two previous Short Courses (and references therein), the following material will be devoted to other proton-related special topics important to spacecraft developers. In the three sections to follow, we first treat two special topics related to the "classic" phenomenology of proton-induced recoil initiated SEEs. Next we treat a relatively recent phenomenon affecting several types of very sensitive devices in which protons can initiate upsets by direct ionization. Finally, the last portion of this section will examine various classes of proton-initiated hard errors.

4.1 Test Issues and Special Cases

The "classic" approach to proton SEE testing of memories involves loading a pattern and setting up desired test conditions, exposing the Device Under Test (DUT) to some predetermined fluence, and interrogating the device to determine level of functionality and changes from the initial test conditions. The exposures may take place either in air or vacuum for high energy (>10 MeV) protons, and it is almost always required, for health safety reasons, that test personnel be remote to the exposure area during irradiations. Usually, the test setup involves test equipment (e.g., memory tester, computer with controller card, transient digitizer, etc.) local to the test and the ability to control that equipment remotely from either an extended monitor and keyboard or across a communication link or network connection.

For devices other than memories, the test instrumentation can become quite complicated. For example, processor tests may require comparison with either a second (ghost) processor or with expected results emulated in software. Such a test usually involves real time monitoring of the DUT during exposure. Often, testing of a given component must be done *in situ* with supporting flight hardware and software to fully assess the impact of SEEs and their likelihood of propagating through the system. This is especially true for circuit implementations incorporating error detection and correction circuitry. Throughout this section, the examples for discussion and case studies have been selected to illustrate not only some of the effects that protons may have, but also the choices and tradeoffs confronting the test engineer in gathering meaningful data without overcomplicating the test effort.

4.1.1 High Speed Technologies: While there still exists some controversy regarding the ability to accurately correlate proton and heavy ion SEE sensitivities, it is generally agreed that protons are more likely to affect technologies which exhibit lower thresholds for heavy ion SEE effects (e.g., LET_{th} below ~10 $MeVcm^2/mg$). By virtue of their lower nodal capacitance and lower switching energies, as well as the absence of a complementary structure, this tends to include several high speed technologies. Protons are known to cause SEEs in Si bipolar devices (ECL), GaAs MESFET and HIGFET devices, GaAs HBT based devices, and other high speed technologies [McMo-96, and references therein]. In general, if the technology has been developed with high speed in mind, then it is likely to be sensitive to proton SEEs, unless SEE hardening has been explicitly incorporated.

For a given component, the effect on the circuit and subsystem can be extremely dependent on how the part functions in the circuit, and how follow-on circuit parameters affect error propagation. Investigations have shown that SEE cross sections in high speed technologies can be very dependent on device clock speeds [Mars-95, Reed-96], and even circuit hardening attempts may exhibit a clock speed dependence [Schn-92]. This is understood in terms of reduced noise margins during switching so that the circuit is more vulnerable to SEEs and that vulnerability occurs more often as the clock speed increases [Reed-96, and references therein].

The combination of inherent SEE softness in high speed logic with the increased sensitivity at high data rates argues for *in situ* proton testing of high speed circuitry where accurate flight error rate predictions are desired. Such testing is conceptually straight forward, but often challenging to carry out. Complications include the need to provide the DUT with high data rate signals and detect errors "on the fly" without being sensitive to the electrically noisy accelerator environment. The requirement to do this remotely argues for test automation with custom software and hardware. Supporting test hardware must itself be capable of the speeds of the DUT, and should in fact have broadband characteristics with ample bandwidth margin. This often requires the design of test circuits that must be fabricated to operate in the GHz regime.

Figure 11 illustrates the test hardware and software environments used in the proton SEE evaluation of a commercial fiber channel transceiver set fabricated in a Si p-ECL process [Cart-97]. The referenced paper describes the DUT and analyzes the test results, but a

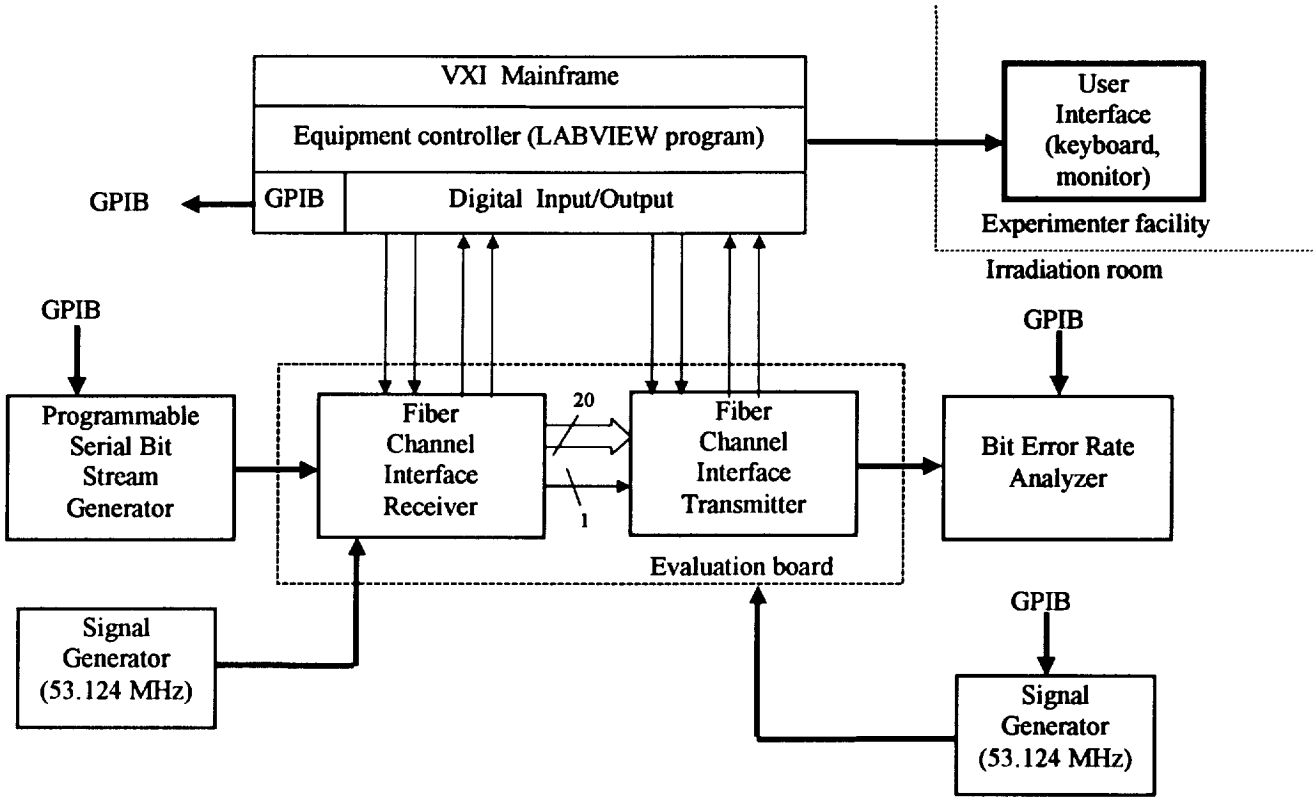

Figure 11. Block diagram for a 1.0625 gigabit per second proton-induced single event effects test of a commercial fiber channel chip set [Cart-97]. Testing required automatic data logging and remote control of both the DUTs and also the bit error rate test equipment.

significant portion of the paper is devoted to the test hardware and methodology with emphasis on the fact that meaningful proton evaluations of high-speed technologies are nontrivial. As the data rates increase into the Gbps regime, availability of state-of-the-art bit error rate test equipment becomes a significant issue. Combined equipment costs can exceed $1M. The test development time and risk associated with transport to accelerator facilities are important concerns.

As identified in figure 11, the test relied on a "VME eXtended for Instrumentation" (VXI) mainframe running LABVIEW® software to control instruments and capture data. Test conditions were set from the VXI chassis via a digital I/O card interface and General Purpose Interface Bus (GPIB). Software controlling the test flow included interfaces to the commercial 12.5 Gbps bit error rate test equipment as well as the custom hardware evaluation boards. During the test, errors were logged automatically and stored on the VXI controller's embedded processor module's hard drive, and simultaneously made available over an Ethernet hub for remote archival storage. The test flow control and software interface were exercised by test personnel using a keyboard and monitor extension, but all high speed test equipment and control equipment had to be placed in the target room. Whenever test equipment must be located near the target it is a good, if not necessary, precaution to be aware of the possibility of scattered protons and neutrons reaching the equipment and place more sensitive units where the exposures will be minimized.

The previous example described the evaluation of a commercially available device that was being considered for flight. Often, the interest is in the proton SEE characteristics of a technology, and test circuits may be used resulting in simplification of DUT interfaces. Examples are described in [Mars-95 and Reed-96] along with data showing the importance of going to the trouble of the high speed test approach. Figure 11a illustrates that significant differences in proton upset sensitivity for static versus dynamic testing can result as the data rates enter the hundreds of Mbps regime. The explanation is based on an enhanced sensitivity as data transitions near clock edges, and this is carefully mapped out in [Reed-96].

In general, it is important to test a device with as much fidelity as possible to the intended application, and this is especially important with regard to clock speed where high data rates are required. Design of test hardware and DUT fixtures for high data rates is challenging in itself, and misleading results can follow from bandwidth-limited test configurations [Reed-96]. For this reason, broadband test sets with excess bandwidth are highly recommended.

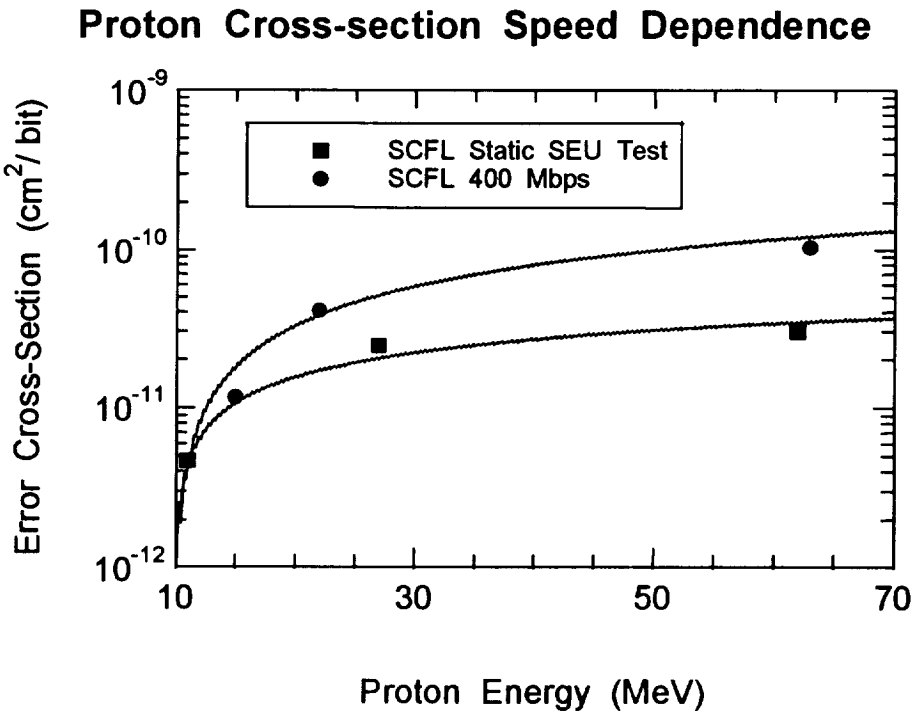

Figure 11a. Bit error rate testing of GaAs HIGFET shift registers showed that static upset measurements would underpredict the upset rates by large factors if the intended application involves fast clock speeds [Mars-95]. These factors increase as the data rates increase and can approach 100.

4.1.2 Small Probability Events: A recent Short Course [Pete-97] pointed out that the total dose sensitivity of a technology can place practical limitations on the accurate determination of proton SEE cross sections. This can be true for TID hardened parts where assurances of very low cross sections are needed, but it may be much more important for COTS or other unhardened devices for which the TID failure levels may be only a few krad(Si). If the TID failure level of a candidate component is on the order of ~10 krad(Si), then testing on an individual DUT will be limited to that dose. If protons of ~60 MeV are used, this corresponds

to a device cross section of ~10^{-11} cm^2. Smaller cross sections cannot be measured with a single device, although they may be important, especially for hard failures and disruptive soft error modes.

The accurate determination of SEE cross sections for important events can require testing of many devices to TID failure levels to get even poor SEE statistics. Such measures may be required when the SEE may lead to catastrophic failure, when many copies of the same device are present on the same satellite, or when many copies of the same device are used in a constellation of identical satellites.

The NASA Hubble Space Telescope offers one such example with its 12 Gbit Solid State Recorder (SSR). The SSR is based on DRAM technology and uses 1440 die with each containing 16 Mbits. Details of the proton SEE response of the individual die are provided in [LaBe-98], along with a description of in-flight anomalies that indicated proton sensitivity. Prior to flight, testing had been performed with both heavy ions and protons and on flight lot die. In these tests, block errors were identified through heavy ion testing, and the LET threshold was measured at about 5 $MeVcm^2/mg$. With such a low threshold, protons might be also be expected to cause block errors, but after 3 flight lot die were tested to proton fluences of ~ 3 x 10^{11} (~30 krad(Si)), the devices failed from TID without exhibiting the single event induced block error.

However, after launch, two block errors were noticed and correlated with the proton environment. To understand the source of the these errors, further analysis pointed to the need for additional proton testing with a larger sample size. After a second round of testing with a sample size of 100 die, it was determined that protons could lead to the block error condition, and 9 such events were noted on the 100 die sample set. Calculations of the error cross section and expected in-flight error rate showed good agreement with the anomaly rate. Fortunately, for the HST case the block errors were easily corrected with robust Reed-Solomon EDAC protection. The details of this example and others are found in [LaBe-98].

If the error condition were not easily corrected, or worse, if permanent failure resulted, the condition would not have been predicted with a small test sample set. When large numbers of a given device are flown either on the same spacecraft or across a large number of satellites, correspondingly large samples sizes must be used to assess all possible SEE modes. The exact number will be a function of both the orbit and the TID response of the DUT. If hard failure modes are possible, then large sample sizes may be warranted, even if only one device is to be flown.

4.1.3 Single Event Transients in Linear Devices: Transient effects in linear circuits were first reported by Koga, et al. in [Koga-93]. Their study examined transient signals that propagate to the output of analog circuits as a result of heavy ion irradiation. The following year, Ecoffet and coworkers confirmed the findings of Koga, et al., and extended the study to examine transients in several linear circuits, including LM 108 operational amplifiers, LM 111 voltage comparators, LM 218H operational amplifiers, and LM 211 voltage comparators [Ecof-94]. Their findings demonstrated the impact of the problem in each of these part types, and more importantly, showed that for some cases the heavy ion LET

threshold for initiating transients can be quite low (e.g. well below 5 MeVcm^2/mg for the LM 108 and LM 111 devices). Ecoffet, et al., point out that such a low threshold would be expected to result in sensitivity to high energy protons.

Nichols, et al., reported proton-induced transients in LM 111 and LM 139 comparators. Their analysis indicated that the transient duration could exceed 200 ns in some cases. Proton error cross sections were on the order of 10^{-10} cm^2 per device over the range from 30 MeV to 200 MeV. Measurements showed varying sensitivity with input voltage levels and also included heavy ion measurements on the same device types. LaBel, et al., have also noted the sensitivity of linear circuits to proton induced transients [LaBe-95a]. Currently, the risk associated with proton induced transients is being assessed by a number of groups. If anything, it is more complex than with digital circuits since the magnitude and duration of the transient vary greatly with several parameters (e.g., input conditions, output loading, proton energy, etc.), and the effects are highly circuit and application dependent.

4.1.4 Correlation Between Proton and Heavy Ion SEE Sensitivities: Before concluding this discussion of "traditional" proton SEE we briefly examine approaches that have been offered to correlate proton SEE with heavy ion SEE. Such correlation can be useful for estimating proton upset sensitivity when heavy ion data is available. In addition, for present technologies, the correlation approaches can allow the estimation of heavy ion sensitivity when only proton data exist or when packaging issues preclude penetration by heavy ions to the active device regions. These estimates can be useful, but if high confidence predictions are required, these estimates should not be substituted for test results from the flight lot devices in application specific test configurations.

PROFIT (for Proton Fit) is an empirical model that allows fitting of heavy ion data or heavy ion data combined with proton test data to extract parameters allowing prediction of proton upset rates [Calv-96]. The approach requires knowledge of the number of sensitive cells. It assumes that sensitive cells have the same spatial dimensions but may have differing critical charge levels. In comparisons with the two-parameter Bendel approach, the referenced paper showed very good agreement for the 18 different device types used in the study.

In [O'Ne-98], another approach based on proton reaction kinematics shows how upper bounds on the heavy ion upset rates and failure probabilities can be estimated from 200 MeV proton data. This correlation requires proton data as input, and can be especially useful when heavy ion data are not available. The method does not allow estimation of proton upset sensitivity from heavy ion data.

The final correlation technique we will discuss was first reported in 1983 and has been revised several times with the most recent being "The SEU Figure of Merit and Proton Upset Rate Calculations" [Pete-98 and references therein]. This approach is based on the claim that upset sensitivity for a given device can be summarized by a single parameter, the figure of merit (FOM). The referenced paper indicates how the FOM can be calculated based on either the heavy ion upset saturation cross section and threshold or from the proton upset saturation cross section. Once determined from either data set, the same FOM can be used to estimate

upset rates from either trapped protons or from heavy ions. The aggregate upset rate will then be the combination of the two contributions. The referenced paper shows good agreement for a variety of device types with varying levels of SEE sensitivity.

In some instances it is of interest to assess neutron SEE sensitivity, such as in avionics applications. In [Norm-98] the Burst Generation Rate (BGR) technique for assessing proton upset sensitivity is compared with neutron BGR calculations and data. If neutron SEE data were available on a device, this approach could be taken to gain an idea of proton upset sensitivity, but as the reference indicates the correlation is not precise. Though it was not mentioned in the introduction where reasons for proton testing were listed, one possibility would be that the assessment with protons could be used with the BGR correlation to estimate neutron SEE sensitivity for avionics applications.

4.2 Proton Direct Ionization and SEEs

The preceding section examined special cases of the conventional indirect proton SEE mechanism, which involves heavily ionizing nuclear reaction recoil products. Until just a few years ago, this was considered to be the only important mechanism for proton-induced single event effects. In several recent studies, SEEs due to direct ionization by protons have been reported. Though these may be "special" cases, their treatment in terms of mechanism identification, test issues, hardening solutions, and rate predictions are unique, and the remainder of this section will address these issues.

At the outset, we note that for the indirect mechanism to occur there must be a reaction, and the reaction cross sections are so low such that only about 1 proton in ten thousand undergoes such an event. Most protons traverse the region and leave only an ionization track, which often matters little. However, if the circuit is sensitive to the amount of charge deposited by a single ionization track from a proton traversal, then the event cross sections may be greatly increased, by up to four orders of magnitude over the indirect mechanism. Such devices will therefore be very likely to exhibit SEEs with high rates in proton environments.

4.2.1 CCDs: In order for a device to be sensitive to direct ionization from protons, it is likely designed for an application requiring high sensitivity. In the case of the charge coupled device imaging array, the sensitivity is required to register faint signals from distant objects. For some applications, the signal may literally be only a few electrons integrated into the imager's depletion volume prior to readout. Not surprisingly, when a proton traverses the same depletion region or nearby material from which the deposited charge can diffuse, the CCD pixel registers a false signal. These false signals from proton SEEs can affect science instruments and star tracker based navigational equipment as well. An excellent reference exists which examines the rates and charge signatures for carefully controlled test conditions and provides orbital predictions for a LEO application in the proton belts [Lomh-90].

There are two techniques to minimize the effects from unwanted proton strikes. Imaging arrays on the NASA HST mission are troubled with these stray signals when in the South Atlantic Anomaly so much that they curtail the science operations when passing

through this high flux region. When stopping operation is not practical, such as with a star tracker, transient events are usually rejected by using a Kalman filter approach to average over several frames of imagery and reject signals which are not repeated in subsequent frames taken in view of the same region.

In figure 12, the four images have been acquired by a 1024 pixel by 1024 pixel CCD incorporated into one of the chronograph instruments on board the Solar and Heliospheric Observarory (SOHO) satellite. SOHO occupies an orbit around the L1 libration point that sits 930,000 miles from the Earth on the Sun-Earth line. The coronagraph instrument filters the bright orb to focus on the details of the coronal structure; hence the dark circles in the center. The four panels depict the development of a coronal mass ejection (CME) on 11/6/97. CMEs and solar flares are the two categories of solar disturbances that can result in solar proton events at satellite positions. The two lower panels show the effects of CME protons reaching the coronagraph's CCD. Even though the instrument has heavy shielding to protect the CCD, the > 100 MeV protons from the CME penetrated to the focal plane. Note the range of proton

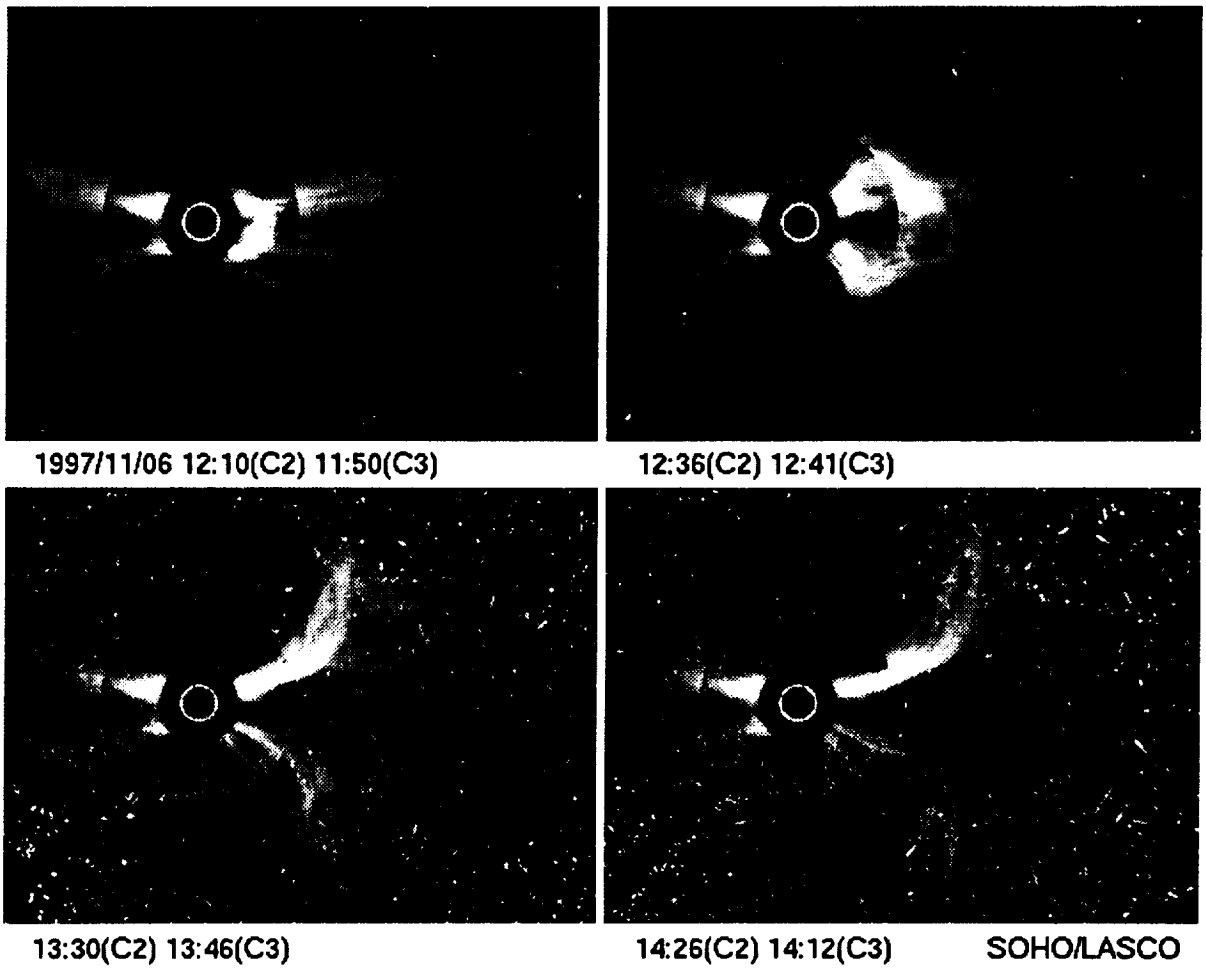

Figure 12. Coronagraphs from the SOHO satellite follow the evolution of a coronal mass ejection. Protons from the event reach the instrument's CCD and "pepper" the image with transients in the lower two panels.

transient sizes and path trajectories indicating apparent omnidirectional arrival. Also note that the images are from different frames, and the proton transients are not repeated in the same image locations. For this reason, temporal filtering techniques can minimize the interference from the proton strikes for star trackers and other applications requiring tracking of bright objects against a cluttered background. More can be found on these images at the website, "sohowww.nascom.nasa.gov".

4.2.2 Optical Link Photodetectors: In recent years several missions have implemented fiber-optic based local area networks for spacecraft telemetry and control busses as well as high data rate payload busses. Data transmission via optical fiber offers advantages in terms of power savings and reduced electromagnetic interference concerns, and these issues become increasingly important at data rates in the Gbps regime. The optical signal level representing a digital "1" may contain very little energy. When received at the link's terminal and converted back to an electrical signal by an optoelectronic photodetector, the signal level may be only a few hundred or thousand electrons prior to amplification. Several studies have demonstrated how the photodetector, by virtue of its low signal level, can be sensitive to false signals from direct ionization by incident protons. For details and additional information, please see the review article [Mars-96, and references therein].

The sensitivity of the photodetector is perhaps not so surprising in view of the fact that this optoelectronic detector functions to capture digital information at rates into the Gbps regime from optical signals with average powers of only a few μW. This results in valid signals of only a few hundred electrons in some cases. Also, the photodiode must necessarily be large enough to capture the optical signal. For typical multimode fiber, this corresponds to surface areas of thousands of square microns (the device examined in our study has a 75 micron optical aperture with an 80 micron diameter junction). Photodiode physical cross sections can easily exceed 10^{-5} cm^2, and due to their extreme sensitivity, the error cross sections can be correspondingly large.

Figure 13 depicts the disk-shaped planar photodiode structure under reverse bias conditions and indicates various particle trajectories that deposit charge by direct ionization. The sketch beneath shows resulting current pulses sensed in the receiver circuit which decay with an RC time constant determined by the circuit bandwidth. Also depicted is the received signal provided in a no-return-to-zero (NRZ) protocol containing the digital information. The ratio between the high and low current levels (the "extinction ratio") is typically about 10. Receiver circuits are almost always designed to accommodate a range of incident average optical powers and automatically adjust the decision level, or threshold, to be midway between the high and low levels. As suggested in the figure, data can be disrupted if ion-induced current exceeding the threshold current is sensed at the critical mid-bit decision when a "0" is being transmitted.

Though the photodiode must be large enough to capture the optical signal, it obviously should be no larger. The analysis indicates better SEE characteristics for III-V direct bandgap detectors since a depletion depth of only about 2-3 microns can result in > 80% quantum efficiency. This is in contrast with indirect bandgap detectors, such as Si for 830 nm applications, in which depletion depths are about twenty times larger. Specifically, the thinner InGaAs structure minimizes both the "target" size for ion strikes as well as the ion

pathlength when hit. Also, the III-V device is characteristic of the design choices being considered for high bandwidth data busses since the thin junction offers minimal capacitance. To take advantage of these benefits, most design efforts use III-V InGaAs detectors for 1300 nm lightwave detection. More recently, 850 nm photodetectors with thin depletion regions and favorable SEE performance have been identified [Mars-98].

4.2.2.1 Proton SEE Measurements on Fiber Optic Receiver Circuits: Proton testing of operating links can be done *in situ* using subsystem hardware or on components using a commercial bit error rate test set. For the purpose of understanding the test approach and underlying mechanisms and their effects, we present the latter approach here. The subsystem hardware level effects can in turn be inferred from this material, and the impact on the subsystem will differ according to the particular protocol and architecture. Examples of the relation between hardware level effects from "generic" device testing and the impact on specific subsystems can be found in [Carts-97, Dale-97, Mars-96, and references therein]. The SEE response of all associated circuitry must be considered, but we focus on bit errors in the photodetector receiver since it is primary importance in many cases.

Figure 14 illustrates a typical test setup for measuring link bit-error-ratio (BER) performance at the component level. The BER is ratio of bits in error to total bits transferred for a given transmission interval. Full details of the measurement are found in [Mars-94a]. This setup for proton testing is similar to that shown in figure 11 for fiber-channel transceiver hardware, and the need for software controlled data collection and logging applies here too.

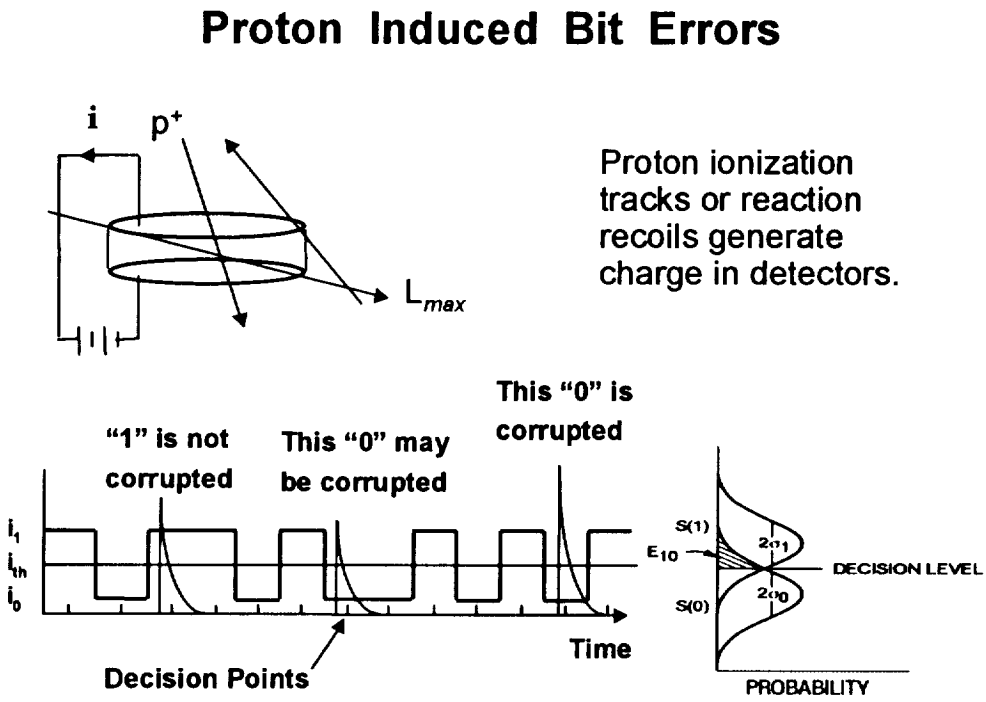

Figure 13. The reverse biased disk-shaped planar collects charge that is deposited by direct ionization from protons. Resulting current pulses sensed in the receiver circuit decay with an RC time constant determined by the circuit bandwidth. Data can be disrupted if ion-induced current exceeding the threshold current is sensed at the critical mid-bit decision when a "0" is being transmitted.

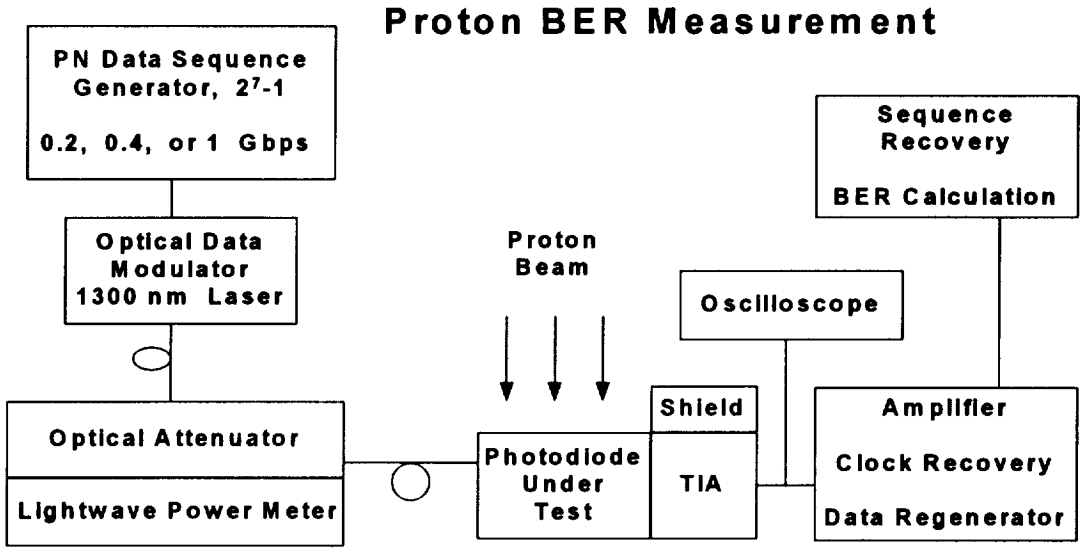

Figure 14. This illustrates a typical test setup for measuring link bit-error-rate performance. Full details of the measurement are found in [Mars-94a]. The automated test set uses commercially available bit error rate test equipment.

The tester was set to generate a serial pseudo random numeric (PN or PRN) sequence of (2^7-1) bits in length. Data rates of 200, 400, and 1000 Mbps were established by an external waveform generator. The fiber link included a programmable attenuator so that the desired optical power level could be adjusted over the range of -30 dBm to 0 dBm (or 1 μW to 1 mW). The optical power was monitored by an external light wave meter or coupled onto the surface of the photodiode under test. Light was launched onto the photodiode using a 3-axis micro-manipulator stage, and coupling efficiency was maximized by tuning and monitoring the photodiode output on a digital sampling oscilloscope. Signals were amplified by a Trans-Impedance Amplifier (TIA) and evaluated for errors resulting from proton strikes.

With protons incident on the photodiode, we monitored the BER and recorded the number of errors. Measurements of BER were typically made with >100 total errors to assure good statistics. This usually covered a time interval of minutes. By logging the percent of error free intervals, we verified that for protons the errors were due to individual events and not contiguous errors from a single strike. Similarly, for higher LET He ions, we determined the average number of errors per strike using this method.

These measurements described here and in [Mars-94a] were performed at the Naval Research Laboratory beam-line (beam-line 2) at the Crocker Laboratory, University of California. For *in situ* measurements of data transmission with bit periods of only a few nanoseconds, one must carefully consider the beam's temporal structure and its relation to the data stream. We examined the impact of the 22 MHz cyclotron frequency (at 63 MeV) which provides micro-pulses of approximately 1.3 ns duration every 44 ns. Our experiments were

conducted in a manner to assure this did not influence bit-error cross section measurements. Consideration of the microstructure of the timing of proton arrivals may be an important experimental issue is some situations [LaBe-93], especially when high data rates are involved. Most high energy proton facilities have similar concerns.

4.2.2.2 Analysis and Indication of the Role of Direct Ionization in Photodetectors: Next we consider the example of errors from proton-induced direct ionization in photodetectors to show that they can be quantified with the well-developed tools used in more conventional single event investigations. As is customary with spatially separated arrays of memory elements in Random Access Memories (RAMs), we define bit error cross sections for temporally separated bits in a data stream as the ratio of failed bits to the particle fluence incident on the device during the interval in which the failures are measured. Our objective is to understand the error cross section dependence on environmental factors such particle flux and also the particle energy and angle of incidence, which impact the *effective* linear energy transfer (LET). Also, for a given receiver design, we measure the cross section dependence on the data link characteristics including the data rate and the optical power incident on the photodiode. The result is a data set that can be readily analyzed with existing descriptions of the expected environment to produce estimates of link performance in orbit.

In [Mars-94a] the case is made for treating link bit errors as arising from direct as opposed to the indirect upset mechanism. Several indications point to this interpretation including the angular dependence of measured cross section data, the relation between ionization induced charge and electrical signal size, the relation between device physical size and the magnitude of the error cross section, and the particle and LET dependence of the measured cross section. Realizing that direct ionization causes upsets has two important implications for rate predictions for proton-induced errors. First, the traditional Bendel approach does not apply, and second, the proper approach should more closely follow the approach developed for heavy ion induced upset based on LET.

Figure 15, and the discussion found in [Mars-94a], show that the proton-induced error data can in fact be usefully viewed as dependent on the effective particle LET, even though the errors are due to protons. The solid lines in the curve follow the customary Weibull form (equation 2), where a, b and c are fitted parameters and σ_{sat} is the saturation cross section of the cross section versus LET relation. The family of Weibull curves corresponds to different levels of optical power used in the operating link. It is important to note that the data of figure 15 correspond to a particular data rate and the LET is for the InGaAs detector material.

$$(LET) = \left[1 - e^{-\left(\frac{LET-a}{b}\right)^c}\right]\sigma_{sat} \qquad [2]$$

To assess proton effects on the link at other data rates, we could analyze other data sets measured at other rates as we have for the 400 Mbps data set. However more general results can be obtained by inspecting figure 16, which plots cross section dependence on

optical power for 200, 400, and 1000 Mbps. The two data sets shown represent the high and low LET particles, namely He ions and high energy protons. Note that across the full optical power range and for these two extremes in particle LET, the cross section exhibits, to first order, a direct proportionality to data rate. This trend was noted in all of the detector BER data, and it is consistent with the arguments pertaining to clock rate dependence made earlier in this section. According to equation 3, a cross section that is proportional to data rate results in a BER which is *independent* of data rate. The cross section is represented by σ, and ϕ is the particle flux. The on-orbit error rate in terms of errors per day, however, would be expected to scale linearly with error cross section. It would be up to the application as to whether the BER or the error rate is the more important metric.

$$\mathrm{BER} = \frac{\#\,\mathrm{errors}}{\mathrm{Bits\ Transmitted}} = \frac{\sigma \cdot \phi}{\mathrm{Data\ Rate}} \qquad [3]$$

By using the Weibull approximation we can describe the LET dependence of the proton-induced error cross section and then combine this response with the LET spectrum arising from direct ionization by protons in the detector material system. Then it is possible to exercise the conventional tools for heavy ion upset rate predictions to assess link BER performance in proton rich orbits. This general approach has been validated against flight data with excellent agreement [LaBe-97a, Mars-96, and references therein].

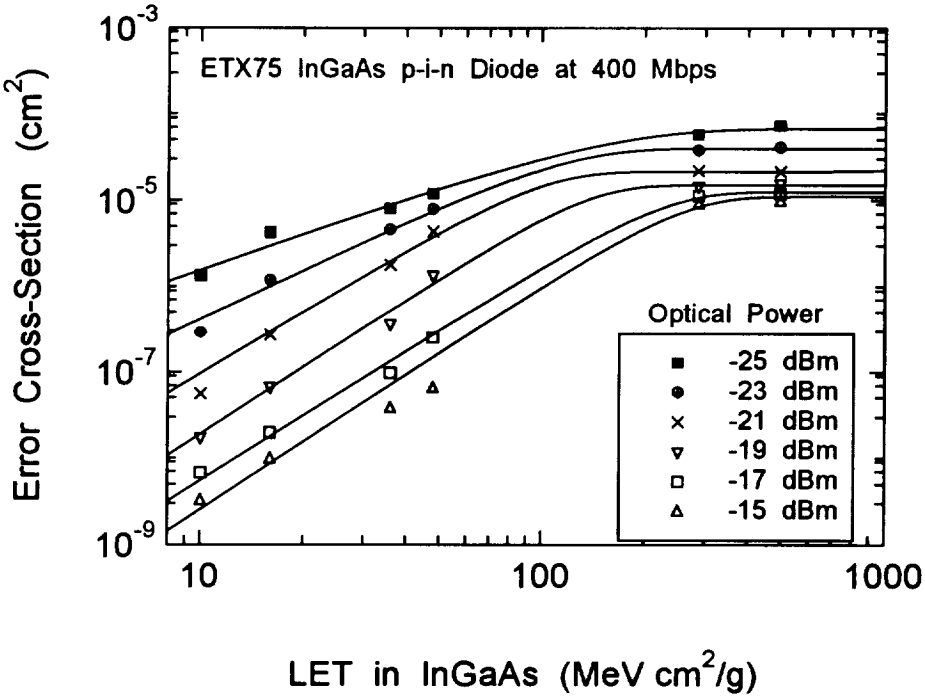

Figure 15. Proton-induced bit error data depends on the effective particle LET, even though the errors are due to direct ionization from protons [Mars-94a],. The solid lines in the curve follow the customary Weibull form, and the family of Weibull curves corresponds to different levels of optical power used in the operating link.

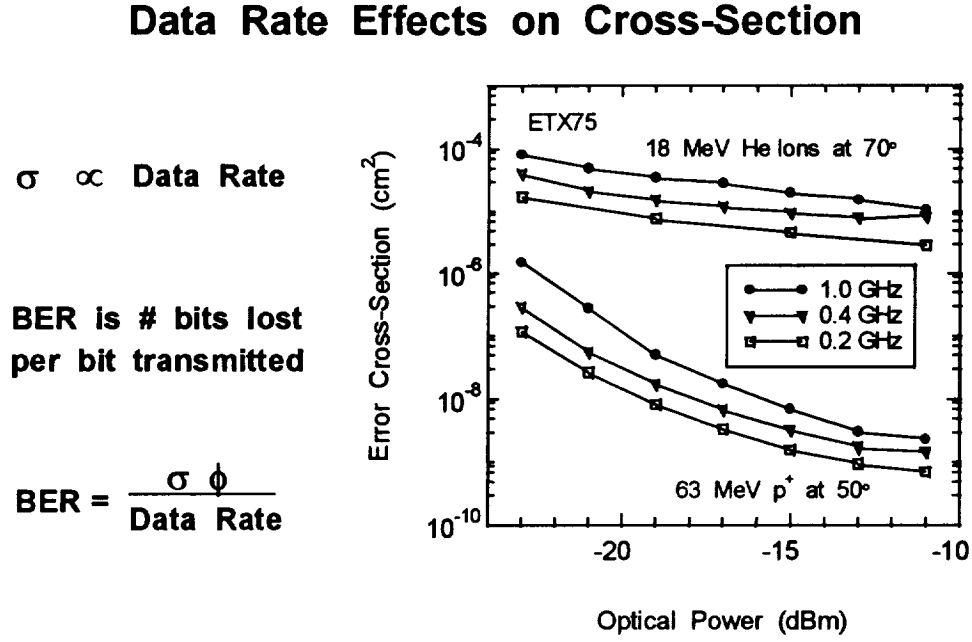

Figure 16. The Bit Error Ratio (BER) cross section for proton strikes on a photodetector is approximately proportional to data rate irrespective of optical power or LET. The relations indicate that a cross section that is proportional to data rate results in a BER which is *independent* of data rate.

4.2.3 Optocouplers and Metal-Semiconductor-Metal (MSM) Photodiodes: The introduction and section 4.1 offered discussion and references to the extensive literature describing "conventional" proton effects involving nuclear reactions and the indirect upset mechanism. The section 4.2 then dealt with a newer formalism that applies to devices that exhibit behavior that is dominated by direct ionization from protons. Not surprisingly, some devices show characteristics of both behaviors. This section examines two such examples.

Optocouplers have received a great deal of attention for their sensitivity to displacement damage from protons and this will be discussed at length in Section IVB on displacement effects. At the 1997 NSREC it was reported that high bandwidth optocouplers could also be sensitive to proton-induced transient effects [LaBe-97]. That study reported that proton initiated transients exhibited a rapid onset and then dissipated with a time constant governed by the bandwidth of the device. At first this appeared to be another example of the general problem of transient effects in linear devices, caused presumably by proton reaction recoil products. But on closer inspection, the angular dependence seen in figure 17 shows an enhancement in the cross section around the plane of the package. For the classic reaction recoil mechanism, no angular dependence would be expected. In [LaBe-97] the explanation is offered in terms of a combination of mechanisms. Figure 18 depicts the situation in which the device response is dominated by strikes to the optocoupler's internal photodetector with nuclear reactions causing transients when they occur, regardless of the angle of incidence. However, for protons traversing the plane of the photodetector sufficient signal can follow from direct ionization across the longer pathlengths.

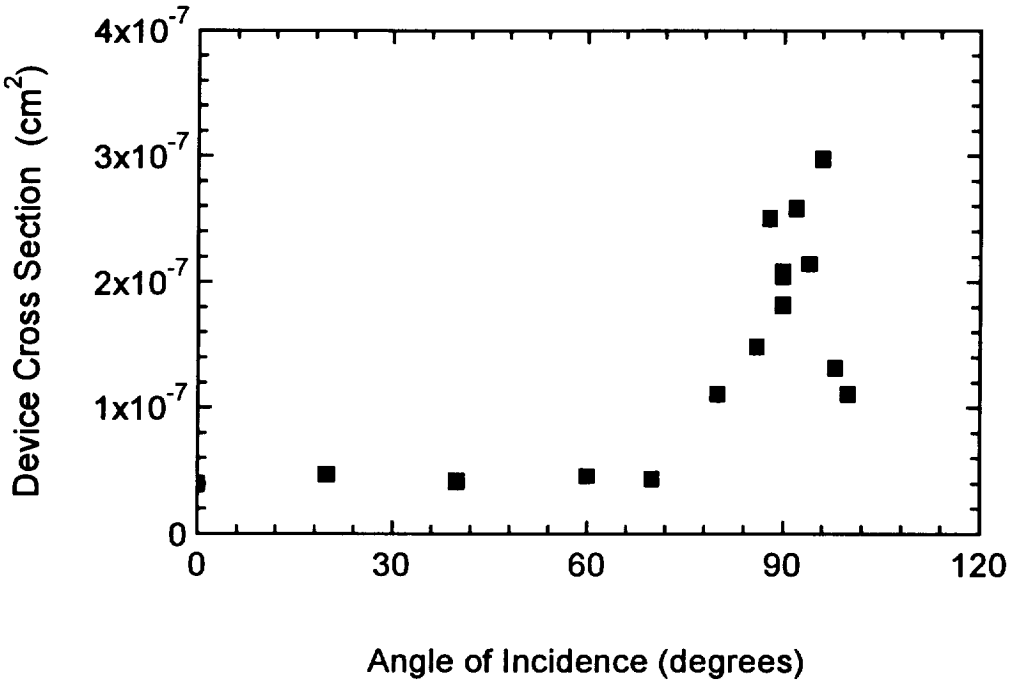

Figure 17. Proton-induced transients in optocouplers exhibit an enhancement in the cross section when the beam is directed in the plane of the package. For the classic reaction recoil mechanism, no angular dependence would be expected. In [LaBe-97] this behavior is explained in terms of a combination of direct ionization through the plane of the photodetector and indirect reaction mechanisms.

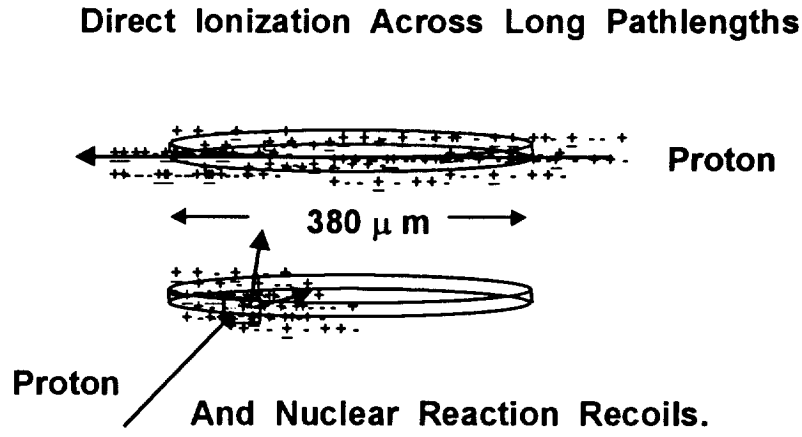

Figure 18. This drawing from [LaBe-97] depicts the situation in which the device response is dominated by strikes to the optocoupler's internal photodetector with nuclear reactions causing transients when they occur, regardless of the angle of incidence. For protons traversing the plane of the photodetector, sufficient signal can follow from direct ionization across the longer pathlengths.

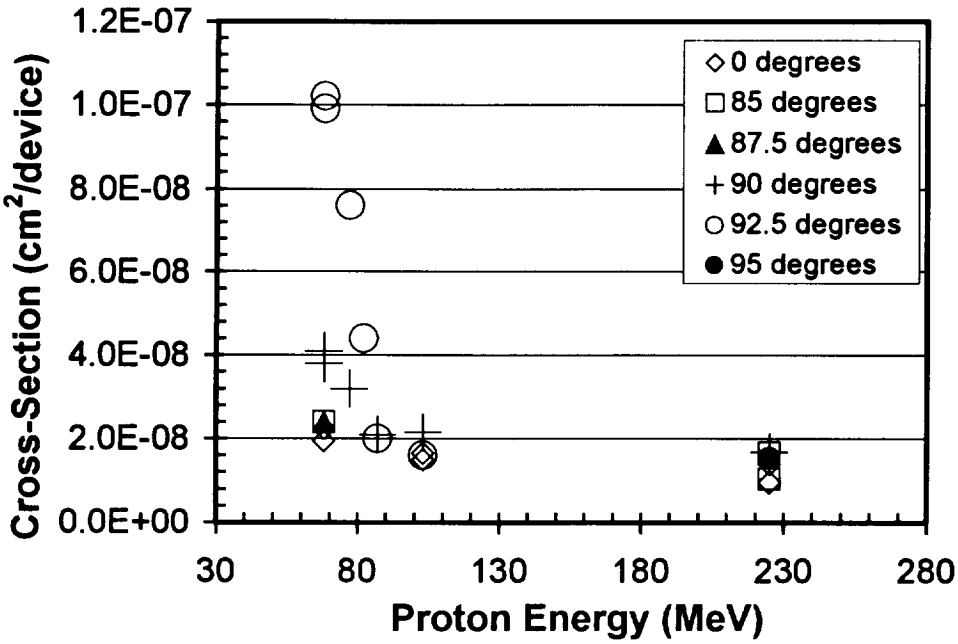

Figure 19. Data supporting the role of the direct ionization mechanism for optocoupler transients shows an apparent LET threshold for the effect [Reed-98]. The increased cross section seen when protons traverse the plane of the diode does not occur with protons above a certain LET (corresponding to ~100 MeV protons).

The following year Reed, et al. reported additional data supporting the role of the direct ionization mechanism in terms of an apparent LET threshold for the effect [Reed-98]. Figure 19, reproduced from that paper, reveals that the increased cross section seen when protons traverse the plane of the diode does not occur with protons above a certain LET (corresponding to ~ 100 MeV). Johnston, et al. extended the study to other devices and included heavy ions as well as protons [John-98]. Their findings suggest that at higher LET's corresponding to cosmic rays the follow-on amplifier circuit may also lead to transient effects, and that for protons the nuclear elastic scattering may be important to the process.

Another study has pointed to the important combination of direct and indirect mechanisms for the case of Metal-Semiconductor-Metal (MSM) photodetectors for use in digital data links such as the fiber-based data busses already described [Mars-98]. The MSM detector technology offers the advantage of a nearly planar geometry which minimizes the pathlengths (and ionization signature) when traversed by protons. Enhanced proton transient cross sections in the plane of the detector and the signature of a threshold LET for direct ionization effects were both noted for MSM devices in [Mars-98].

The existence of multiple mechanisms for transient effects has important implications for the methods and accuracy of transient rate predictions. It has been suggested [LaBe-97] that the aggregate transient rate must be calculated as the sum of the rates for indirect effects using the Bendel formalism plus the direct contribution using the modified RPP approach and measured Weibull-type LET dependence as described for photodetectors in the previous section. For devices exhibiting large enhancements in the cross section near the plane of the

device as in figure 18, both mechanisms are obviously important, and the dominant one would depend on the details of the application and the environment. It should be assumed that the rates would depend on how such a device is operated in terms of expected signal levels and detection sensitivity.

4.3 Destructive Failures

The concerns for TID failure and soft errors treated in the last two sections are serious issues for designers, but the possibility of an unrecoverable catastrophic failure from a single particle event ranks among the highest concerns. Where cosmic ray heavy ions are present, proton-induced hard failures may not be the dominant threat from the natural environment; however, these failure modes should not be overlooked. In the three sections below on Single Event Latch-up (SEL), Single Event Burnout (SEB), and stuck bits, we examine the various ways in which proton-induced single events can render a circuit unusable.

4.3.1 Latch-Up (and COTS): We first consider SEL with the recognition that it is not solely a COTS issue, but it is a major concern when using COTS CMOS parts in space. Latch-up in CMOS devices is well understood in terms of a particle-induced triggering of an SCR action in a parasitic p-n-p-n path. Details of the mechanism, modeling tools, hardening approaches, and references to related topics are in covered in the NSREC Short Course Notes from 1996 [John-96]. It should be noted that not all latch-up modes lead to destructive failure, and in some cases power cycling may be used to restore nominal operating conditions.

For many years, SEL was considered to be a CMOS phenomenon only in cosmic ray environments, but at the 1992 NSREC two papers reported first the laboratory confirmation of proton-induced latch-up [Nich-92] and the observation of a proton-induced latch-up event in space [Adam-92]. In these studies, the affected CMOS devices were either on a bulk or a thick epitaxial substrate, and the corresponding heavy ion latch-up threshold was fairly low (below 10 MeVcm^2/mg). Even so, the proton energy threshold below 50 MeV for both cases suggests that proton-induced latch-up may be a higher risk than cosmic ray induced latch-up in mid-latitude LEO applications.

Since 1992 there have been many examples of proton-induced latch-up, both in the laboratory and in-flight. Table 2 has been reproduced from [Norm-98] where it was compiled to show several examples from the literature as the basis for evaluating his formulation of the Burst Generation Rate (BGR) model for predicting latch-up sensitivity in microprocessors. Note the K-5 processor results as fabricated on the 2 micron thick epitaxial material. This is one of the more unexpected results, and it is noted, though not explained, in the original reference [John-97]. Both of these papers, and references therein, note the general correlation between susceptibility to heavy ion induced latch-up with low LET threshold, and the sensitivity to proton-induced latch-up. The lack of a more quantitative correlation is blamed on the differences between charge deposition by heavy ions and proton-induced recoils and the associated charge collection processes [John-97].

For crude estimates, it is probably reasonable to assume that devices which exhibit a low heavy ion latch-up threshold (below 5 MeVcm^2/mg) will also be sensitive to proton-

induced latch-up and even devices with LET thresholds of twice that may be suspect. The K5 example also illustrates that fabrication on a thin epitaxial starting material does not necessarily guard against latch-up, though systematic study of varying epi-layer thickness in one process has shown this to be an important step toward hardening against latch-up [LaBe-95]. Conversely, it is probably a safe assumption that if a device has been demonstrated to be hard or immune to latch-up by heavy ions then it will show similar hardness with respect to protons.

Table 2: Measured and Calculated Proton SEL Cross Sections

Device	Measr'd Proton SEL X-Section, cm^2	BGR Calct'd Proton SEL X-Section, cm^2	Re-marks	Ref. for Data
HM65162	1.4E-10	1.4E-10		31
NEC-4464	1.8E-10	1.5E-10		32
K-5	6.6E-9	2.2E-11	t=6μm	32
K-5	6.6E-9	4E-9	t=2μm	32
LSI-64811	1.7E-11	6E-12		32
LCA200K	1.4-4.1E-11	7.6E-11		8
XC96002	4.5E-9	2.6E-10	t=6μm	33
XC96002	4.5E-9	8.8E-9	t=4μm	33
IDT3081	3E-11	0.9E-11		34

More detailed discussion of the present understanding of the mechanisms and modeling for proton-induced SEL can be found in the references provided. In general, even if knowledge of a thin epitaxial material suggests latch-up immunity, latch-up testing should be performed prior to consideration for flight application when the process under question is not well known. Heavy ion screening would be a first step with proton latch-up testing advised only if the heavy ion threshold were low and there was a need to quantify the risk in a proton rich environment. In practice, most missions would avoid the use any part susceptible to failure by proton-induced latch-up for a critical application based on the risk to heavy ion induced failure alone.

4.3.2 Proton-induced Single Event Burnout (SEB) in Power MOSFETs: Single event burnout occurs when an ion or proton-induced recoil atom strikes a power MOSFET in its "off" state and triggers a parasitic bipolar junction transistor. This "on" transistor creates a conduction path between source and drain, and the resulting regenerative feedback leads to a high current state causing second breakdown and burnout. Single event burnout in power MOSFETs has received considerable attention as a hard failure mode from heavy ion effects [Titu-96, Alle-96, Ober-96, Adol-96, and references therein]. Recently, as was the case with latch-up, both experimental investigations and in-flight experience have pointed to protons as a possible cause for burnout. Two 1996 NSREC papers addressed this issue, one with laboratory measurements [Ober-96] and the other with flight data [Adol-96].

Oberg and co-authors evaluated the response of power MOSFETs to both high-energy proton and to high energy neutron irradiation [Ober-96]. Their evidence indicated some correlation between proton SEB cross sections and those for neutrons and heavy ions, with the

more energetic protons being more likely to cause burnout. The flight data from the CRUX experiment [Adol-96] both confirmed the effect for orbital protons and showed it to be more likely on the higher voltage (200 V) device, as expected. Figure 20 shows additional flight data and correlation of SEB rate with the applied voltage on the CRUX experiment that appear in [Bart-98]. The bias dependence is expected based on electric field dependence of the problem as described in [Titu-96, and references therein].

If proton-induced hard failure is possible, then heavy ion induced hard failure would also be possible. The determination of which failure mode would be more likely depends on the particle environment internal to the satellite and on the relative sensitivities of the device in question. [Bart-98] compares two sets of power MOSFETS flown on the CRUX experiment and shows that on a given satellite, proton-induced burnout may dominate for one device while heavy ion burnout dominates for another. In practice, power MOSFET applications typically de-rate the devices to improve reliability, avoid gate rupture, and prevent burnout. With proper de-rating, the threat of proton-induced burnout can be avoided.

4.3.3 Stuck Bits: The key paper introducing this topic was presented by Oldham, et al., in 1993 with the title "Total Dose Failures in Advanced Electronic from Single Ions," [Oldh-93]. Their work describes the ability of a single ion to deposit sufficient energy along its path to result in localized increases in trapped oxide charge and interface state generation. In fact, for small feature sizes, an entire transistor gate can be affected and undergo failure as a result of localized dose deposition and threshold voltage shift. The initial work in DRAMs resulted in bits which could not be rewritten, hence the term "stuck bits". This effect can occur in any device type, and is not just a problem for memories. Their paper also points out the expected increasing importance of this problem with decreasing feature size, and this has since been observed. The following year, Poivey, et al. expanded the study in terms of device types, ion species, and analysis. In that paper, the more formal term "Single Hard Error (SHE)" was introduced [Poiv-94].

At present, proton-induced stuck bits are not considered to be a significant problem, though scaling trends suggest that this may soon change. Proton-induced stuck bits may be either temporary or permanent as reported in [Sore-95]. Figure 21, from the CRUX experiment, indicates that stuck bits have occurred in all device types included in the experiment. Though they have been correlated with solar particle events, [Bart-98] points out that most events have been outside of the SAA and therefore are more likely due to heavy ions.

From a test perspective, it is common to see stuck bits during proton SEE testing as the TID limit of the technology is approached. That, along with increased leakage currents, is an indication of the need to resume the test with a fresh device.

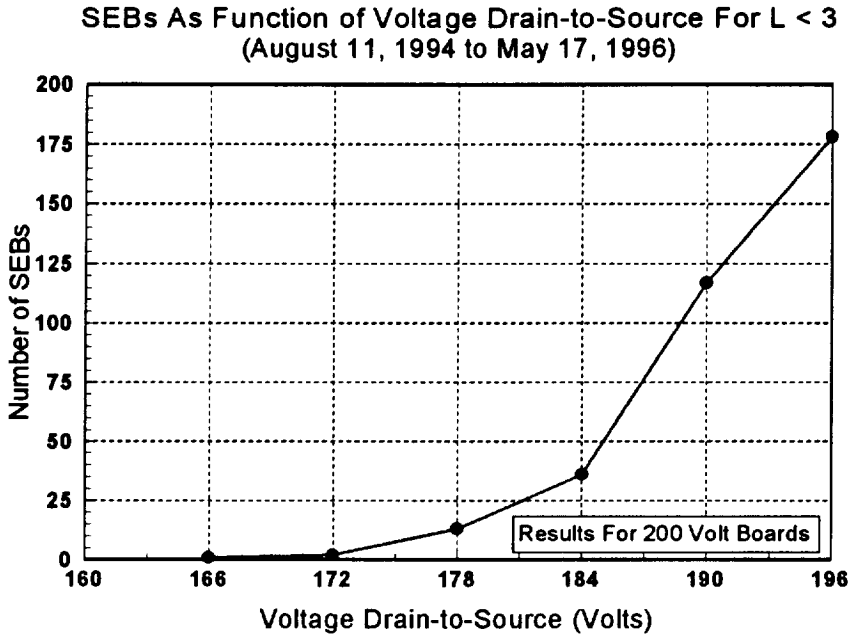

Figure 20. The results of the power MOSFET single event burnout experiment flying on CRUX confirm that protons can lead to device failure and showed that the proton rates can exceed heavy ion induced SEB rates [Bart-98].

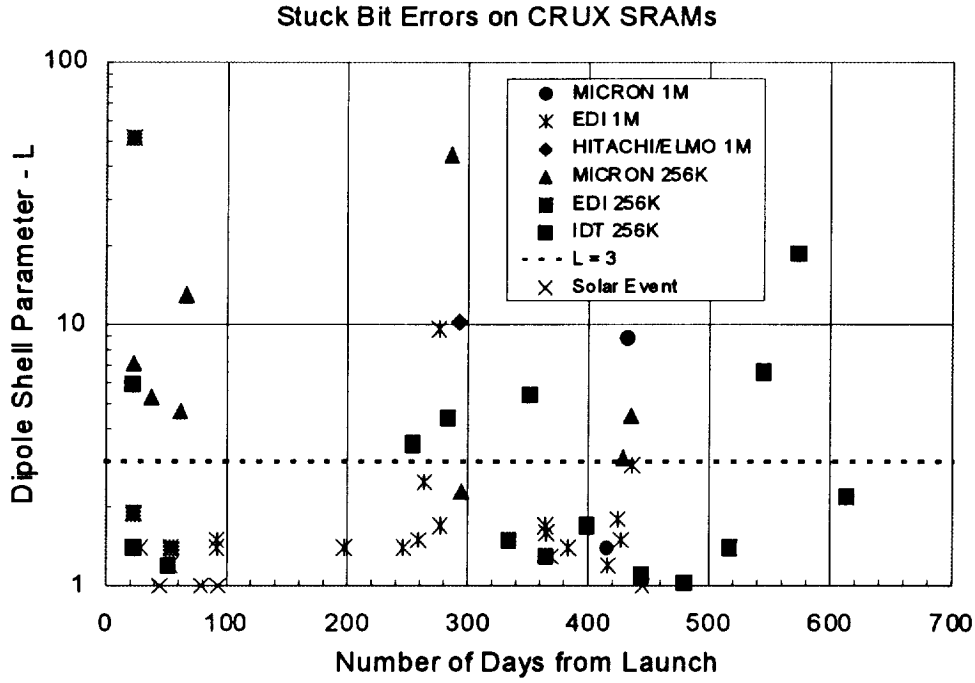

Figure 21. Stuck bits have occurred in all the modern memory devices flying on the CRUX experiment [Bart-98]. The chart indicates that some (for L < 3) are probably due to protons, but most are thought to be heavy ion related.

5.0 SUMMARY

Satellite microelectronic and photonic devices subjected to the ionizing effects of protons may exhibit responses either from total ionizing dose or from single event phenomena. Heavily shielded devices will likely receive dose primarily from protons in orbits encountering the inner radiation belts. For total ionizing dose, we have reviewed the literature comparing the equivalence of proton dose versus other sources of dose deposition found in either the space environment or in laboratory test facilities. We conclude that Co-60 and electron dose satisfactorily simulate proton dose for most purposes.

Many different single event phenomena arise from protons including soft errors from nuclear inelastic reaction events, nuclear scattering events, and even direct ionization in several types of more sensitive devices. Special considerations are needed for SEU testing of high speed devices and for evaluations of devices with low soft error cross sections relative to their TID failure levels. In addition, both destructive and nondestructive hard errors may result from proton-induced reactions. In many cases, the concern for hard errors will be greater for cosmic rays, but in geomagnetically shielded (e.g., low-Earth orbits) the greater risk can be proton-related.

Satellite subsystem design efforts benefit from proper expression of the anticipated proton environments in thorough requirements aimed at describing realistic typical and worst case proton flux and fluence levels. We have discussed many aspects of the environment models and their associated uncertainties as they affect the requirement definition.

6.0 ACKNOWLEDGMENTS

We gratefully acknowledge partial support, technical suggestions, and complete encouragement from our colleagues and friends in the Radiation Effects and Analysis Group and Radiation Physics Office at NASA Goddard Space Flight Center. We also appreciate the helpful interactions with the Radiation Effects Branch members at the Naval Research Laboratory and throughout the radiation effects community.

7.0 REFERENCES FOR INTRODUCTION AND PART A

(All references are unclassified.)

[Adam-92] L. Adams, E.J. Daly, R. Harboe-Sorensen, R. Nickson, J. Haines, W. Schafer, M. Conrad, H. Griech, J. Merkel, T. Schwall, and R. Henneck, "A Verified Proton-Induced Latch-up in Space," IEEE Trans. Nucl. Sci., Vol. 39, No. 6, pp. 1804-1808, 1992.

[Adol-96] John W. Adolphsen, Janet L. Barth, and George B. Gee, "First Observation of Proton-Induced Power MOSFET Burnout in Space: The CRUX Experiment on APEX," IEEE Trans. Nucl. Sci., NS-43, No. 6, pp. 2921-2926, 1996.

[Alle-96] M. Allenspach, C. Dachs, G.H. Johnson, R.D. Schrimpf, E. Lorfevre, J.M. Palau, J.R. Brews, K.F. Galloway, J.L. Titus, and C.F. Wheatley, "SEGR and SEB in N-Channel Power MOSFETS," IEEE Trans. Nucl. Sci., NS-43, No. 6, pp. 2927-2937, 1996.

[Augu-82] L.S. August, "Estimating and Reducing Errors in MOS Dosimeters Caused by Exposure to Different Radiations," IEEE Trans. Nucl. Sci., Vol. 29, No. 6, pp. 2000-2003, 1982.

[Bart-97] Janet Barth, "Modeling Space Radiation Environments," Notes from the 1997 IEEE Nuclear and Space Radiation Effects Conference Short Course, 1997.

[Bart-98] Janet L. Barth, John W. Adolphsen, and George B. Gee, "Single Event Effects on Commercial SRAMS and Power MOSFETS: Final Results of the CRUX Flight Experiment on APEX," 1998 IEEE Radiation Effects Data Workshop Record, pp. 1-10.

[Bend-84] W.L Bendel and E.L. Petersen, "Predicting Single Event Upsets in the Earth's Proton Belts," IEEE Trans. Nucl. Sci., Vol. 31, No. 6, pp. 1201-1207, 1984.

[Calv-96] Philippe Calvel, Catherine Barillot, and Pierre Lamonthe, "An Empirical Model for Predicting Proton Induced Upset," IEEE Trans. Nucl. Sci., NS-43, No. 6, pp. 2827-2832, 1996.

[Cart-97] M.A. Carts, P.W. Marshall, C.J. Marshall, K.A. LaBel, M. Flanegan, and J. Bretthauer, "Single Event Test Methodology and Test Results of Commercial Gigabit per Second Fiber Channel Hardware," IEEE Trans. Nucl. Sci., NS-44, No. 6, pp. 1878-1884, 1997.

[Ecof-94] R. Ecoffet, S. Duzellier, P. Tastet, C. Aicardi, and M. Labrunee, "Observation of Heavy Ion Induced Transients in Linear Circuits," IEEE NSREC Radiation Effects Data Workshop Record, pp. 72-77, 1994.

[Feyn-96] J. Feynman and S.B. Gabriel, "High Energy Charged Particles in Space at One Astronomical Unit," IEEE Trans. Nucl. Sci, Vol. 43, No. 2, pp. 344-352, 1996.

[Frie-88] R.K. Frietag, E.A. Burke, C.M. Dozier, and D.B. Brown, "The Development of Non-Uniform Deposition of Holes in Gate Oxides," IEEE Trans. Nucl. Sci., NS-35, No. 6, pp. 1203-1207, 1988.

(All references are unclassified.)

[Gate-96] Michele Gates, Kenneth A. LaBel, Janet Barth, Allan Johnston, and Paul W. Marshall, "Single Event Effects Criticality Analysis," NASA Report, See NASA GSFC Radiation Effects & Analysis Home Page, http://flick.gsfc.nasa.gov/radhome.htm, 1996.

[Guen-79] C.S. Guenzer, E.A. Wolicki, and R.G. Allas, "Single Event Upset in Dynamic RAMs by Neutrons and Protons," IEEE Trans. Nucl. Sci., NS-26, No. 6, pp. 5048-5055, 1979.

[Hous-98] S.L. Houston and K.A. Pfitzer, "A New Model for the Low Altitude Trapped Proton Environment," IEEE Trans. Nucl. Sci., Vol. 45, No. 6, pp. 2972-2978, 1998.

[IEEE-1156] IEEE P1156.4, "Standard for Environmental Specifications for Spaceborne Computer Modules," 1995.

[Ingu-97] C. Inguimbert, S. Duzellier, R. Ecoffet, and J. Bourrieau, "Proton Upset Rate Simulation by a Monte Carlo Method: Importance of the Elastic Scattering Mechanism," IEEE Trans. Nucl. Sci., Vol. 44, No. 6, pp. 2243-2249, 1997.

[John-96] Gregory H. Johnson and Kenneth F. Galloway, "Catastrophic Single Event Effects in the Natural Radiation Environment," Section IV from the 1996 IEEE Nuclear and Space Radiation Effects Conference Short Course Notes.

[John-97] A.H. Johnston, G.M. Swift, and L.D. Edmonds, "Latchup in Integrated Circuits from Energetic Protons," IEEE Trans. Nucl. Sci., Vol. 44, No. 6, pp. 2367-2377, 1997.

[John-98] A.H Johnston, G.M. Swift, T. Miyahira, S. Guertin, and L.D. Edmonds, "Single Event Upset Effects in Optocouplers," IEEE Trans. Nucl. Sci., Vol. 45, No. 6, pp. 2867-2875, 1998.

[Kinn-98] James D. Kinnison, "Achieving Reliable, Affordable Systems," Section V from the 1998 IEEE Nuclear and Space Radiation Effects Conference Short Course Notes.

[Koga-93] R. Koga, S.D. Pinkerton, S.C. Moss, D.C. Mayer, S. LaLumondiere, S.J. Hansel, K.B. Crawford, and W.R. Crain, "Observation of SEUs in Analog Microcircuits," IEEE Trans. Nucl. Sci., NS-40, No. 6, pp. 1838-1844, 1993.

[LaBe-93] Kenneth A. LaBel, Paul Marshall, Cheryl Dale, Christina Crabtree, E.G. Stassinopolous, Jay T. Miller, and Michele M. Gates, "SEDS MIL-STD-1773 Fiber Optic Data Bus: Proton Irradiation Test Results and Spaceflight SEU Data," IEEE Trans. Nucl. Sci., Vol. 40, No. 6, pp. 1638-1645, 1993.

[LaBe-95] K.A. LaBel, Donald K. Hawkins, J.A. Kinnison, W.P. Stapor, P.W. Marshall, "Single Event Effect Characteristics of CMOS Devices Employing Various epi-Layer Thicknesses," IEEE Proc. of RADECS, 95TH8147, pp. 258-262, Sep 1995.

[LaBe-95a] K.A. LaBel, A.K. Moran, D.K. Hawkins, A.B. Sanders, E.G. Stassinopoulos, R.K. Barry, C.M. Seidlick, H.S. Kim, J. Forney, P.Marshall, and C. Dale, "Single Event Effect Proton and Heavy Ion Test Results in Support of Candidate NASA Programs," NSREC Radiation Effects Data Workshop, pp. 16-32, 1995.

(All references are unclassified.)

[LaBe-97] Kenneth A. LaBel, Paul Marshall, C.J. Marshall, M. D'Ordine, M. Carts, G. Lum, H.S. Kim, C.M. Seidleck, T. Powell, R. Abbott, J. Barth, and E.G. Stassinopolous, "Proton Induced Transients in Optocouplers: In-flight Anomalies, Ground Irradiation Test, Mitigation and Implications," IEEE Trans. Nucl. Sci., Vol. 44, No. 6, pp. 1885-1892, 1997.

[LaBe-97a] K.A. LaBel, P.W. Marshall, C.J. Marshall, J. Barth, H. Leidecker, R. Reed, and C.M. Seidlick, "Comparison of MIL-STD-1773 Fiber Optic Data Bus Terminals: Single Event Proton Test Irradiation, In Flight Performance, and Prediction Techniques," Proceedings of RADECS 97, pp. 332-338, 1997.

[LaBe-98] K.A. LaBel, P.W. Marshall, J.L. Barth, R.B. Katz, R.A. Reed, H.W. Leidecker, H.S. Kim, and C.J. Marshall, "Anatomy of an Anomaly: Investigation of Proton Induced SEE Test Results for Stacked IBM DRAMs," IEEE Trans. Nucl. Sci., Vol. 45, No. 6, pp. 2898-2903, 1998.

[Lomh-90] T.S. Lomheim, R.M. Shima, J.R. Angione, W.F. Woodward, D.J. Asman, R.A. Keller, and L.W. Schumann, "Imaging Charged-Coupled Device (CCD) Transient Response to 17 and 50 MeV Proton and Heavy Ion Irradiation," IEEE Trans. Nucl. Sci., Vol. 37, No. 6, pp. 1876-1885, 1990.

[Ma-89] Ionizing Radiation Effects in MOS Devices and Circuits, T.P. Ma and Paul V. Dressendorfer, John Wiley and Sons, New York: 1989.

[Mars-94] Paul W. Marshall, Cheryl J. Dale, E. Joseph Friebele, and Kenneth LaBel, "Survivable Fiber-Based Data Links for Satellite Radiation Environments," SPIE Critical Review CR-50 on Fiber Optic Reliability and Testing, 1994.

[Mars-94a] Paul W. Marshall, Cheryl J. Dale, Martin A. Carts, and Kenneth A. LaBel, "Particle Induced Bit Erors in High Performance Fiber Optic Data Links for Satellite Data Management," IEEE Trans. Nucl. Sci., NS-41, No. 6, pp. 1958-1965, 1994.

[Mars-95] Paul W. Marshall, Cheryl J. Dale, Todd R. Weatherford, Michael La Macchia, and Kenneth A. LaBel, "Particle Indiced Mitigation of SEU Sensitivity in High Data Rate GaAs HIGFET Technologies," IEEE Trans. Nucl. Sci., NS-42, No. 6, pp. 1844-1854, 1995.

[Mars-95a] Paul W. Marshall, Cheryl J. Dale, Martin E. Fritz, Michael de La Chapelle, Martin A. Carts, and Kenneth A. LaBel, "Total ionizing dose and single particle effects in a 200 Mbps star-coupled fiber optic data bus," Proc. of SPIE Conference on Photonics for Space Environments III, Proc. # 2482, 1995.

[Mars-96] P.W. Marshall, C.J. Dale, and Kenneth A. LaBel, "Space Radiation Effects in High Performance Fiber Optic Data Links for Satellite Data Management," IEEE Trans. Nucl. Sci. NS-43, Vol. 2, p. 645 (1996).

(All references are unclassified.)

[Mars-98] C.J. Marshall, P.W. Marshall, M.A. Carts, R.A. Reed, and K.A. LaBel, "Proton Induced Effects in a Metal-Semiconductor-Metal (MSM) Photodetector for Optical Based Data Transfer," IEEE Trans. Nucl. Sci., NS-45, No. 6, pp. 2842-2848, 1998.

[McMo-96] D. McMorrow, T.R. Weatherford, S. Buchner. A.R. Knudson, J.S. Melinger, L.H Tran, and A.B. Campbell, "Single Event Effects in GaAs Devices and Circuits," IEEE Trans. Nucl. Sci., NS-43, No. 2, pp. 628-624, 1996.

[Meff-94] J.D. Meffert and M.S. Gussenhoven, CRESSPRO Documentation, PL-TR-94-2218, Phillips Laboratory, Hanscom AFB, Mass., 1994.

[Nich-92] Donald K. Nichols, James R. Coss, R. Kevin Watson, Harvey R. Schwartz, and Ronald L. Pease, "An Observation of Proton Induced Latch-up," IEEE Trans. Nucl. Sci., Vol. 39, No. 6, pp. 1654-1657, 1992.

[Nich-96] D.K. Nichols, James R. Coss, Tetsuo F. Miyahira, and Harvey R. Schwartz, "Heavy Ion and Proton Induced Single Event Transients in Comparitors," IEEE Trans. Nucl. Sci., NS-43, No. 6., pp. 2960-2967, 1996.

[Norm-98] Eugene Normand, "Extensions of the Burst Generation Rate Method for Wider Applications to Proton/Neutron Induced Single Event Effects," IEEE Trans. Nucl. Sci., NS-45, No. 6, pp. 2904-2914, 1998.

[Ober-96] D.L. Oberg, J.L. Wert, E. Normand, P.P. Majewski, and S.A. Wender, "First Observations of Power MOSFET Burnout with High Energy Neutrons," IEEE Trans. Nucl. Sci., NS-43, No. 6, pp. 2913-2920, 1996.

[Oldh-83] T.R. Oldham and F.B. McLean, "Charge Collection Measurements for Heavy Ions Incident on n- and p-Type Silicon," IEEE Trans. Nucl. Sci., NS-30, No. 6, pp. 4493-4500, 1983.

[Oldh-84] T.R. Oldham, "Analysis of Damage in MOS Devices in Several Radiation Environments," IEEE Trans. Nucl. Sci., NS-31, No. 6, pp. 1236-1241, 1984.

[Oldh-93] T.R. Oldham, K.W. Bennett, J. Beaucour, T. Carriere, C. Poivey, and P Garnier, "Total Dose Failure in Advanced Electronics from Single Ions," IEEE Trans. Nucl. Sci., NS-41, No. 6, pp. 1820-1830, 1993.

[O'Ne-98] P.M. O'Neill, G.D. Badhwar, and W.X. Culpepper, "Internuclear Cascade-Evaporation Model for LET Spectra of 200 MeV Protons Used for Parts Testing," IEEE Trans. Nucl. Sci., NS-45, No. 6, pp. 2467-2474, 1998.

[Peas-99] Ronald L. Pease, private communication.

[Pete-96] E.L. Petersen, "Approaches to Proton Single Event Rate Calculations," IEEE Trans. Nucl. Sci., NS-43, No. 2, pp. 496-505, 1996.

[Pete-97] E.L. Petersen, "Single Event Analysis and Prediction," Section III, 1997 NSREC Short Course Notes.

(All references are unclassified.)

[Pete-98] E.L. Petersen, "The SEU Figure of Merit and Proton Upset Rate Calculations," IEEE Trans. Nucl. Sci., NS-45, No. 6, pp. 2550-2562, 1998.

[Poiv-94] C. Poivey, T. Carriere, J. Beaucour, and T.R. Oldham, "Characterization of Single Hard Errors (SHE) in 1 M-bit SRAMs from Single Ion," IEEE Trans. Nucl. Sci., NS-42, No. 6, pp. 2235-2239, 1994.

[Reed-96] R.A. Reed, M.A. Carts, P.W. Marshall, C.J. Marshall, S. Buchner, M. LaMacchia, B. Mathes, and D. McMorrow, "Single Event Upset Cross Sections at Various Data Rates," IEEE Trans. Nucl. Sci., NS-43, No. 6, pp. 2862-2867, 1996.

[Reed-98] R.A. Reed, P.W. Marshall, A.H. Johnston, J.L. Barth, C.J. Marshall, K.A. LaBel, M. D'Ordine, H.S. Kim, and M.A. Carts, "Emerging Optocoupler Issues with Energetic Particle Induced Transients and Permanent Radiation Degradation," IEEE Trans. Nucl. Sci., NS-45, No. 6, pp. 2833-2841, 1998.

[Sawy-76] Donald M. Sawyer and James I. Vette, "AP-8 Trapped Proton Environment for Solar Maximum and Solar Minimum," National Science Data Center Report NSSDC/WDC-A-R&S 76-06, 1976.

[Schn-92] R. Schneiderwind, D. Krening, S. Buchner, K. Kang, and T.R. Weatherford, "Laser Confirmation of SEU Experiments in GaAs MESFET Combinational Logic," IEEE Trans. Nucl. Sci., NS-39, No. 6, pp. 1665-1670, 1992.

[Selt-80] Stephen Seltzer, "SHIELDOSE: A Computer Code for Space-Shielding Radiation Dose Calculations," National Bureau of Standards (NBS) Technical Note 1116, May, 1980.

[Shim-89] Y. Shimano, T. Goka, S. Kuboyama, K. Kawachi, T Kanai, and Y. Takami, "The Measurement and Prediction of Proton Upset," IEEE Trans. Nucl. Sci., Vol. 36, No. 6, pp. 2344, 1989.

[SSP-30512] SSP 30512 Rev. C, "Space Station Ionizing Radiation Design Environment," June, 1994.

[Sore-95] R. Harboe-Sorensen, R. Muller, and S. Frenkel, "Heavy Ion, Proton and Co-60 Radiation Evaluation of 16 Mbit DRAM Memories for Space Application, 1995 IEEE Radiation Effects Data Workshop, pp. 42-49.

[Stap-85] W.J. Stapor, L.S. August, D.H. Wilson, T.R. Oldham, and K.M. Murray, "Proton and Heavy Ion Radiation Damage Studies in MOS Transistors," IEEE Trans. Nucl. Sci., Vol. 32, No. 6, pp. 4399-4404, 1985.

[Stap-90] W.J. Stapor, J.P. Meyers, J.B. Langworthy, and E.L. Petersen, "Two Parameter Bendel Model Calculations for Predicting Proton Induced Upset," IEEE Trans. Nucl. Sci., Vol. 37, No. 6, pp. 1966-1972, 1985.

[Stap-95] William J. Stapor, "Single Event Effects Qualification," Section II, 1995 IEEE NSREC Short Course Notes.

(All references are unclassified.)

[Stass-88] E.G. Stassinopoulos and J.P Raymond, "The Space Radiation Environment for Electronics," Proc. IEEE, vol. 76, pp. 1423-1442, 1988.

[Stass-90] E.G. Stassinopoulos, "Radiation Environments in Space," in Notes for the 1990 IEEE Nuclear and Space Radiation Effects Conference Short Course, 1990.

[Titu-96] J.L. Titus and C.F. Wheatley, "Experimental Studies of Single Event Gate Rupture and Burnout in Vertical Power MOSFETs," IEEE Trans. Nucl. Sci., Vol. 43, No. 2, pp. 533-545, 1996.

[Titu-98] J.L. Titus and C.F. Wheatley, "Proton Induced Dielectric Breakdown in Power MOSFETs," IEEE Trans. Nucl. Sci., NS-45, No. 6, pp. 2891-2897, 1998.

[Tylk-96] Allan J. Tylka, James H Adams, Jr., P.R. Boberg, Buddy Brownstein, William F. Dietrich, Erwin O. Flueckiger, Edward L. Petersen, Margaret A. Shea, Don F. Smart, and Edward C. Smith, "CREME96 A Revision of the Cosmic Ray Effects on Micro-Electronics Code," IEEE Trans. Nucl. Sci., Vol. 43, No. 6, pp. 2150-2160, 1996.

[Tylk-96a] A.J. Tylka, W.F. Dietrich, P.R. Boberg, E.C. Smith, and J.H. Adams, Jr., "Single Event Upsets Caused by Solar Energetic Heavy Ions," IEEE Trans. Nucl. Sci., Vol. 43, No. 6, pp. 2758-2766, 1996.

[Xaps-89] M.A. Xapsos, R.K. Frietag, E.A. Burke, C.M. Dozier, D.B. Brown, and G.P. Summers, "The Random Nature of Energy Deposition in Gate Oxides," IEEE Trans. Nucl. Sci., Vol. 36, No. 6, pp. 1896-1903, 1989.

[Xaps-90] M.A. Xapsos, private communication.

[Xaps-98] M.A. Xapsos, G.P. Summers, and E.A. Burke, "Probability Model for Peak Fluxes of Solar Proton Events," IEEE Trans. Nucl. Sci., Vol. 45, No. 6, pp. 2948-2953, 1998.